

Efferent Connections of the Internal Globus Pallidus in the Squirrel Monkey: I. Topography and Synaptic Organization of the Pallidothalamic Projection

MAMADOU SIDIBÉ,¹ MARK D. BEVAN,² J. PAUL BOLAM,² AND YOLAND SMITH^{1,3*}

¹Centre de Recherche en Neurobiologie, Hôpital de l'Enfant-Jésus, and Université Laval, Québec, Canada G1J 1Z4

²MRC Anatomical Neuropharmacology Unit, Oxford, OX1 3QT, United Kingdom

³Division of Neuroscience, Yerkes Regional Primate Research Center, and Department of Neurology, Emory University, Atlanta, Georgia 30322

ABSTRACT

The objectives of this study were, on one hand, to better understand how the segregated functional pathways from the cerebral cortex through the striatopallidal complex emerged in the projections to the thalamus and, on the other hand, to compare the ultrastructure and synaptic organization of the pallidal efferents to the ventrolateral (VL) and centromedian (CM) thalamic nuclei in primates. These aims were achieved by injections of the retrograde-antegrade tracer, biotinylated dextran amine (BDA), in different functional regions of the internal pallidum (GPi) in squirrel monkeys. The location of retrogradely labelled cells in the striatum was determined to ascertain the functional specificity of the injection sites.

Injections in the ventrolateral two-thirds of the GPi (group 1) led to retrograde labelling in the postcommissural region of the putamen ("sensorimotor striatum") and plexuses of labelled fibers in the rostral one-third of the principal ventrolateral nucleus (VLp) and the central part of the CM. On the other hand, injections in the dorsal one-third (group 3) and the rostromedial pole (group 4) of the GPi led to retrogradely labelled cells in the body of the caudate nucleus ("associative striatum") and the ventral striatum ("limbic striatum"), respectively. After those injections, dense plexuses of anterogradely labelled varicosities were found in common thalamic nuclei, including the parvocellular ventral anterior nucleus (VApc), the dorsal VL (VLd), and the rostromedial part of the parafascicular nucleus (PF). In the caudal two-thirds of the CM/PF, the labelled fibers formed a band that lay along the dorsal border of the complex in a region called the dorsolateral PF (PFdl) in this study. The ventromedial nucleus (VM) was densely labelled only after injections in the rostromedial GPi, whereas the dorsal part of the zona incerta was labelled in both groups. At the electron microscopic level, the BDA-positive terminals in the VLp were larger and more elongated than those in the CM but, overall, displayed the same pattern of synaptic organization. Our findings indicate 1) that some associative and limbic cortical information, which is largely processed in segregated corticostriatopallidal channels, converges to common thalamic nuclei and 2) that the PF is a major target of associative and limbic GPi efferents in monkeys. *J. Comp. Neurol.* 382:323-347, 1997. © 1997 Wiley-Liss, Inc.

Indexing terms: pallidum; centromedian nucleus; ventrolateral thalamic nucleus; electron microscopy; primate

It is well established that the cerebral cortex imposes upon the primate striatum a compartmentalization into three largely segregated functional territories: 1) the sensorimotor territory, which is represented by the postcommissural putamen, receives afferents from motor and somatosensory cortical areas (Kemp and Powell, 1970; Künzle, 1975, 1977; Jones et al., 1977; Liles and Updyke,

Grant sponsor: Medical Research Council of Canada; Grant numbers: MT-13007, MT-11237; Grant sponsor: NATO; Grant number: CRG 890578; Grant sponsor: National Institute of Health; Grant number: RR00165.

*Correspondence to: Dr. Yoland Smith, Division of Neuroscience, Yerkes Regional Primate Center, Emory University, 954 Gatewood Road NE, Atlanta, GA 30329. E-mail: yolands@rmy.emory.edu

Received 1 February 1996; Revised 6 January 1997; Accepted 21 January 1997

1985; Flaherty and Graybiel, 1991, 1993); 2) the associative territory, which includes the caudate nucleus, is mainly innervated by associative cortical areas (Goldman and Nauta, 1977; Yeterian and Van Hoesen, 1978; Van Hoesen et al., 1981; Selemon and Goldman-Rakic, 1985; Yeterian and Pandya, 1991, 1993); and 3) the limbic territory, which is represented by the rostroventral part of the caudate nucleus and the putamen as well as the nucleus accumbens, receives most of its cortical inputs from limbic-related cortices (Yeterian and Van Hoesen, 1978; Selemon and Goldman-Rakic, 1985; Kunishio and Haber, 1994; Haber et al., 1995). Various pieces of evidence indicate that the functional segregation of corticostriatal projections is maintained largely through the circuitry of the basal ganglia (for reviews, see Alexander et al., 1986; Alexander and Crutcher, 1990). At the level of the pallidal complex, the ventrolateral two-thirds, the dorsal one-third, and the rostromedial pole of the internal pallidum (GPi) receive afferents arising, respectively, from striatal territories innervated predominantly by sensorimotor, associative, and limbic cortical areas (Smith and Parent, 1986; Haber et al., 1990). So far, the assumption that this functional segregation was maintained in the ventrolateral thalamus relied upon data obtained after lesions or injections of anterograde tracers that involved large areas of the GPi, which, unequivocally, included different functional territories (Nauta and Mehler, 1966; Kuo and Carpenter, 1973; Kim et al., 1976; DeVito and Anderson, 1982; Ilinsky and Kultas-Ilinsky, 1987). A first objective of the present study, therefore, was to reexamine the topography of the pallidothalamic projection to the ventrolateral nuclear complex in monkeys, taking into consideration the fact that the afferents from different functional territories of the striatum remain largely segregated at the level of the GPi. This was achieved by means of the anterograde transport of biotinylated dextran amine (BDA; Brandt and Apkarian, 1992; Veenman et al., 1992).

The centromedian nucleus/parafascicular nucleus (CM/PF) intralaminar nuclear complex is another target of pallidal efferents in the thalamus of primates (Nauta and Mehler, 1966; Kuo and Carpenter, 1973; Kim et al., 1976; Harnois and Filion, 1982; Parent and DeBellefeuille, 1983; Hazrati and Parent, 1991) and nonprimates (Carter and Fibiger, 1978; Nauta, 1979; Larsen and Sutin, 1978;

Harnois and Filion, 1982). The majority of GPi cells that project to the CM/PF send axon collaterals to the ventrolateral nucleus (Harnois and Filion, 1982; Parent and DeBellefeuille, 1983). In contrast to the ventral nuclear group, which projects to the cerebral cortex, the major target of CM/PF efferents is the striatum (Parent et al., 1983; Beckstead, 1984; Jayaraman, 1984; Royce and Mourey, 1985; Royce, 1987; Smith and Parent, 1986; Fénelon et al., 1990; Sadikot et al., 1992a,b; Smith et al., 1994; Sidibé and Smith, 1996). The CM and the PF send massive projections that arborize in a complementary fashion in the striatum: The CM innervates predominantly the sensorimotor striatal territory, whereas the PF is related to the associative and limbic striatal regions (Sadikot et al., 1989, 1992a,b; François et al., 1991). Although both the CM and the PF give rise to the thalamostriatal projection, most of the anatomical studies indicate that the efferents of the GPi remain confined to the CM in monkeys (Nauta and Mehler, 1966; Kuo and Carpenter, 1973; Kim et al., 1976). An exception was the observations of DeVito and Anderson (1982), who found labelling in the PF after injections of radioactive amino acids in the dorsal part of the GPi in rhesus monkeys. This discrepancy may have been due to the lack of specificity of the injection sites in the GPi and the lack of information relating to the functional compartmentalization of the CM/PF nuclear complex. The second objective of our study, therefore, was to examine in more detail the pattern of distribution of afferents from different regions of the GPi to the CM/PF complex in the squirrel monkey.

Although the ultrastructural features and synaptic organization of pallidal boutons have been well studied in the ventrolateral nucleus of cats (Kultas-Ilinsky et al., 1983), data obtained in monkeys are still preliminary (Ilinsky et al., 1993; Kayahara and Nakano, 1996). Moreover, the only data available on the synaptic organization of the pallidal input to the CM were those obtained in early anterograde degeneration studies (Harding, 1973; Grofova and Rinivik, 1974; Harding and Powell, 1977). The third objective of this study, therefore, was to analyze the pattern of synaptic articulation between GPi terminals and thalamic neurons in the ventrolateral nuclear group and the CM in the squirrel monkey. The results of this study have been presented in an abstract form (Sidibé et al., 1995).

Abbreviations

AC	anterior commissure	Per or per	neuronal perikaryon
AV	anteroventral nucleus	PF	parafascicular nucleus
Ax	axon	PFdl	parafascicular nucleus, dorsolateral part
CD	caudate nucleus	PU	putamen
CeM	central medial nucleus	Rt	reticular nucleus
CM	centromedian nucleus	STN	subthalamic nucleus
den	dendritic shaft	TH	thalamus
FLt	lenticular fasciculus	VA	ventral anterior nucleus
FR	fasciculus retroflexus	VAmc	ventral anterior nucleus, magnocellular part
GPe	globus pallidus, external segment	VApC	ventral anterior nucleus, parvocellular part
GPi	globus pallidus, internal segment	VL	ventrolateral nucleus
H	field of Forel	VLa	ventrolateral nucleus, anterior part
IC or Ic	internal capsule	VLd	ventrolateral nucleus, dorsal part
III	third ventricle	VLp	ventrolateral nucleus, principal part
LD	laterodorsal nucleus	VLx	ventrolateral nucleus, region X
LV	lateral ventricle	VM	ventromedial nucleus
MD	mediodorsal nucleus	VS	ventral striatum
MT	mammillothalamic tract	Zi	zona incerta
PC	paracentral nucleus		

MATERIALS AND METHODS

Animals and preparation of tissue

Nine adult male squirrel monkeys (*Saimiri sciureus*) were used in the present study. They were anesthetized with a mixture of ketamine hydrochloride (Ketaset; 70 mg/kg i.m.) and xylazine (10 mg/kg i.m.) before being fixed in a stereotaxic frame. The depth of anesthesia was determined by monitoring heart rate, respiration rate, and muscle tone as well as corneal and toe-pinch reflexes. The surgery, anesthesia, and postoperative care were performed according to the guidelines of the Canadian Council on Animal Care and the National Institutes of Health. The BDA (Molecular Probes, Eugene, OR; 5% in distilled water) was loaded in glass micropipettes with a tip diameter ranging from 20 μm to 30 μm . It was then injected iontophoretically into the GPi with a 5 μA positive current for 20 minutes by using a 7 seconds on/7 seconds off cycle. The stereotaxic coordinates were chosen according to the atlas of Emmers and Akert (1963). During the first 2 days after the surgery, the animals received injections of analgesic (buprenorphine, 0.01 mg/kg s.c.) twice daily.

After 7–10 days, the animals were deeply anesthetized with an overdose of pentobarbital (50 mg/kg i.v.) and perfuse fixed with 500–700 ml of cold, oxygenated Ringer's solution followed by 1.5 liters of fixative containing a mixture of 3% paraformaldehyde and 0.5% glutaraldehyde in phosphate buffer (PB; 0.1 M), pH 7.4. This was followed by 1 liter of cold PB. After perfusion, the head was placed in the stereotaxic head holder, and the brain was sliced into 10-mm-thick transverse slabs according to the coordinates of the stereotaxic atlas of Emmers and Akert (1963). The blocks were kept in cold phosphate-buffered saline (PBS; 0.01 M), pH 7.4, until sectioning into 60- μm -thick transverse sections with a vibrating microtome. The sections were collected in cold PBS and treated for 20 minutes with sodium borohydride (1% in PBS). After repeated washes in PBS, they were processed for the histochemical localization of BDA in the light and electron microscope.

Histochemical localization of BDA

In each case, series of adjacent sections throughout the entire extent of the thalamus were processed as follows: 1) histochemical localization of BDA for light microscopic observations, 2) Nissl staining with cresyl violet, 3) histochemical localization of BDA and counterstaining with thionin, and 4) histochemical localization of BDA for electron microscopic analysis.

BDA histochemistry for light microscopy

The first and third series of sections were incubated for 12–16 hours at room temperature with avidin-biotin-peroxidase complex (ABC; Vector Laboratories; 1:100 dilution) in PBS containing 0.3% Triton X-100 and 1% bovine serum albumin (BSA; Sigma Chemical Company). They were then washed in PBS and Tris buffer (0.05 M), pH 7.6, before being placed in a solution containing 3,3'-diaminobenzidine tetrahydrochloride (DAB; 0.025%; Sigma Chemical Company), 0.01 M Imidazole (Fisher Scientific, Nepean, Ontario, Canada), and 0.006% hydrogen peroxide for 10–15 minutes. The reaction was stopped by repeated washes in PBS. The first series of sections was then mounted on chrome alum/gelatin-coated slides, dehydrated, and a coverslip was applied with Permount. The third series of sections was counterstained with thionin to facilitate the

delineation of the thalamic nuclei and to ascertain the location of the labelled terminals.

BDA histochemistry for electron microscopy

The fourth series sections was processed for the visualization of BDA at the electron microscopic level. The sections were placed in a cryoprotectant solution (PB, 0.05 M, pH 7.4, containing 25% sucrose and 10% glycerol) for 20–30 minutes. After sinking, they were frozen at -80°C for 20 minutes. They were then thawed and washed many times in PBS before being processed to localize BDA according to the protocol described above, except that Triton X-100 was not included in the solutions, and the incubation in the ABC was carried out at 4°C for 48 hours. The peroxidase bound to the BDA was localized with DAB.

Processing for electron microscopy

The sections were washed in PB (0.1 M), pH 7.4, before being postfixed in osmium tetroxide (1% solution in PB) for 20 minutes. They were then dehydrated in a graded series of alcohol and propylene oxide. Uranyl acetate (1%) was added to the 70% ethanol (30 minutes) to improve the contrast in the electron microscope. The sections were then embedded in resin (Durcupan ACM; Fluka) on microscope slides and put in the oven for 48 hours at 60°C . After a detailed examination of these sections in the light microscope, regions of interest were drawn and sometimes photographed, then cut from the slides, and glued on the top of resin blocks with cyanoacrylate glue. Serial ultrathin sections were then cut on a Reichert-Jung Ultracut E ultramicrotome and collected on Pioloform-coated, single-slot copper grids. They were stained with lead citrate (Reynolds, 1963) and examined in a Phillips EM300 electron microscope.

Analysis of the material

The location of the BDA injection sites and the resulting retrograde and anterograde labelling were charted by using a Nikon light microscope equipped with a drawing tube. In each case, the anterogradely labelled elements were charted through the entire rostrocaudal extent of the thalamus and the zona incerta. The nomenclature used for the parcellation of the ventrolateral motor thalamic nuclei (Fig. 1) was that recently introduced by Stepniewska et al. (1994a) for New World monkeys. Four representative sections at the level of the ventral anterior nucleus/ventral lateral nucleus (VA/VL; Fig. 1) and three sections at the level of the CM/PF (Fig. 3) were chosen in each case for the schematic illustration shown in Figures 5–8 and 10. The anteroposterior coordinates were determined according to the atlas of Emmers and Akert (1963).

The electron microscopic data were obtained from two cases in which dense anterograde labelling occurred in the principal ventrolateral nucleus (VLp) and the CM. The ultrastructural features and postsynaptic targets of BDA-positive terminals were determined by scanning ultrathin sections enriched in labelled terminals. Each labelled bouton was examined in two to five serial sections, photographed, and enlarged to a final magnification of $\times 20,000$. Their maximum diameter was then measured at the level where the synaptic specialization was the longest by using a computerized image-analysis system and the Ultimage (Graftek, France) software prepared for Macintosh computers. The diameter of the dendritic shafts contacted by labelled

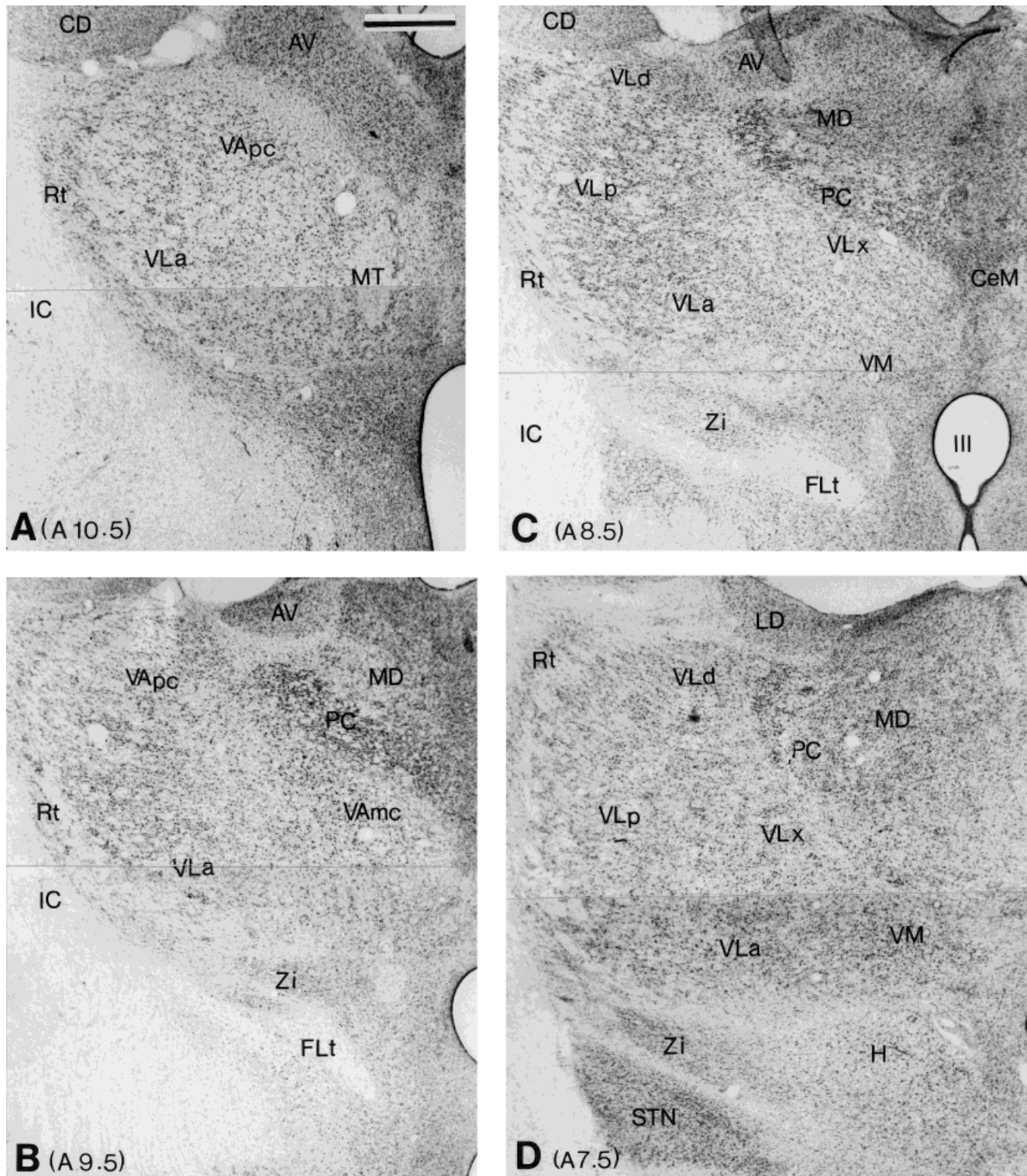


Fig. 1. **A-D**: Series of Nissl-stained transverse sections showing the cytoarchitecture of the ventral anterior/ventral lateral (VA/VL) nuclear complex in the squirrel monkey. The different subnuclei were named according to the nomenclature of Stepniewska et al. (1994a).

The anteroposterior stereotaxic coordinates indicated in the lower left corner of each micrograph were determined according to the atlas of Emmers and Akert (1963). For abbreviations, see list. Scale bar = 1 mm.

boutons was measured by using the same approach. The boutons from the two cases were pooled.

RESULTS

Location of BDA injection sites and retrograde labelling in the striatum

The BDA injection sites in the GPi were characterized by a central core containing many neurons that appeared to be completely filled with the tracer. At the periphery, the intensity of labelling was less dense, so that individual cells filled with BDA could be discerned. The size of the injections extended from 1.0 mm to 2.0 mm in the rostrocaudal and mediolateral planes. Although the tracer slightly leaked along the pipette track in the cases that received injections in the ventral part of the GPi (Figs. 5A, 6A, 8A), it remained confined to the pallidal complex and did not involve significantly the internal capsule (Figs. 5A, 6A, 7A, 8A).

The experimental cases were pooled in four groups according to the location of the injection sites in the GPi and the distribution of retrogradely labelled cells in the striatum: group 1: injections in the ventrolateral two-thirds of the GPi, retrograde labelling in the postcommissural putamen (three cases; Fig. 5A,A'); group 2: injections in the ventromedial part of the GPi located 0.5 mm more rostral and more medial than the injections in group 1, retrograde labelling the ventrolateral part of the precommissural putamen (two cases; Fig. 6A,A'); group 3: injections in the dorsal one-third of the GPi, retrograde labelling in the head and body of the caudate nucleus and in the dorsomedial part of the putamen (three cases; Fig. 7A,A'); and group 4: injections in the rostromedial pole of the GPi, retrograde labelling in the ventral striatum (three cases; Fig. 8A,A').

Nomenclature of thalamic nuclei

According to the nomenclature of Stepniewska et al. (1994a), the VA/VL is divided into seven subnuclei that are distinguished on the basis of the size, shape, and density of neuronal perikarya as well as by the intensity of Nissl staining associated with the component neurons (Fig. 1). Although the exact limit between the subnuclei may be difficult to visualize at low magnification (Fig. 1), the neurons in each subnucleus possess cytoarchitectonic characteristics that distinguish them from their neighbors (Fig. 2). The cytoarchitectonic appearance of these thalamic nuclei was described in detail by Stepniewska et al. (1994a). Examples of neurons that compose the subnuclei that receive most of the GPi efferents are shown in Figure 2. In brief, the parvocellular ventral anterior nucleus (VApc), which represents the rostralmost target of pallidal axons, contains multipolar neurons that are larger and more sparsely distributed than those in the anterior ventrolateral nucleus (VLa; Fig. 2A,C,D). Nevertheless, the precise border between the rostral pole of the VLa and the VApc remains difficult to locate. Two distinguishable features of VLa neurons are the oval shape and small size of their perikarya as well as their arrangement in clusters (Fig. 2B,D). The neurons in the VLp resemble those in the VApc, but they are much more sparsely distributed among a multitude of fiber bundles (Fig. 2B,E). The dorsal ventrolateral nucleus (VLd) is easily distinguishable from the VLp by its higher neuronal density and its lack of large fiber bundles (Fig. 2F).

Three other nomenclatures have been introduced for the terminology of the subdivisions of motor thalamic nuclei in primates (Olszewski, 1952; Jones, 1985; Ilinsky and Kultas-Ilinsky, 1987). To facilitate the comparison of our data with those obtained in previous studies, it is important to note the correspondences between these terminologies, although the delineation of thalamic nuclei is not always based on the same criteria. Overall, the *VLa* and the rostral part of the *VLp* in our study corresponds to the *VLo* of Olszewski (1952), the *VLa* of Jones (1985), and the *VAdc* of Ilinsky and Kultas-Ilinsky (1987). On the other hand, the caudal tier of the *VLp* (not shown in this study) corresponds to the *VPLo* of Olszewski (1952). In the nomenclature of Jones (1985), the *VLp* is a much larger cell group that includes the *VLp*, region X of the ventrolateral nucleus (*VLx*), and the *VLd* identified in our study (Fig. 1). According to the terminology of Ilinsky and Kultas-Ilinsky (1987), the *VLp* is part of a larger complex named the *VL*. The *VLd* and the ventromedial nucleus (*VM*) shown in our study bear the same name in the nomenclature of Ilinsky and Kultas-Ilinsky (1987) but correspond, respectively, to the *VLC* and the *VLM* of Olszewski (1952) or the *VLp* and the *VMP* of Jones (1985).

On the basis of the location of GPi efferents combined with cytoarchitectonic differences in Nissl-stained sections, we subdivided the CM/PF nuclear complex into three parts (Fig. 3). The PF was identified as the medialmost region of the complex that contains densely packed, small, round perikarya (Fig. 3). This nucleus can be easily differentiated from the CM, which is located more laterally, contains a lower density of cells, and is paler in Nissl-stained preparations (Fig. 3). In the middle one-third and the caudal one-third of the nuclear complex, we identified a third subnucleus that we referred to as the dorsolateral part of the PF (*PFdl*). This region is characterized by densely packed, fusiform perikarya oriented in the mediolateral plane (Fig. 3B–D,F). The distinction between this nucleus and the medialmost region of the PF or the underlying CM is clear in Nissl-stained material (Fig. 3B–F).

Anterograde labelling in the thalamus

Morphology of anterogradely labelled fibers in the VA/VL and the CM/PF. The anterogradely labelled fibers that emerged from the injection sites in the GPi followed a common route to reach the thalamus. Numerous BDA-positive fibers coursed in a lateromedial direction to reach the medial pole of the GPi. At this level, the fibers crossed the basis of the internal capsule and accumulated into the lenticular fasciculus, where they formed a compact bundle. Several fascicles detached from the main bundle to reach the subnuclei of the VA/VL rostrally and the CM/PF complex caudally. In the different components of the VA/VL, the GPi fibers displayed common morphological features, i.e., long and thick axonal segments that bore large varicosities (Fig. 4). In most of the subnuclei, the labelled varicose fibers aggregated in the form of glomeruli-like plexuses, whereas, in the *VLp*, they displayed a band-like pattern (Figs. 5–9). In many cases, large varicosities arising from the same axon were apposed on the perikarya and proximal dendrites of individual neurons.

At the level of the CM/PF complex, the labelled fibers displayed morphological features that resembled those of the VA/VL, except that the varicosities were smaller (Fig. 11). In general, the fibers that reached the CM/PF, but

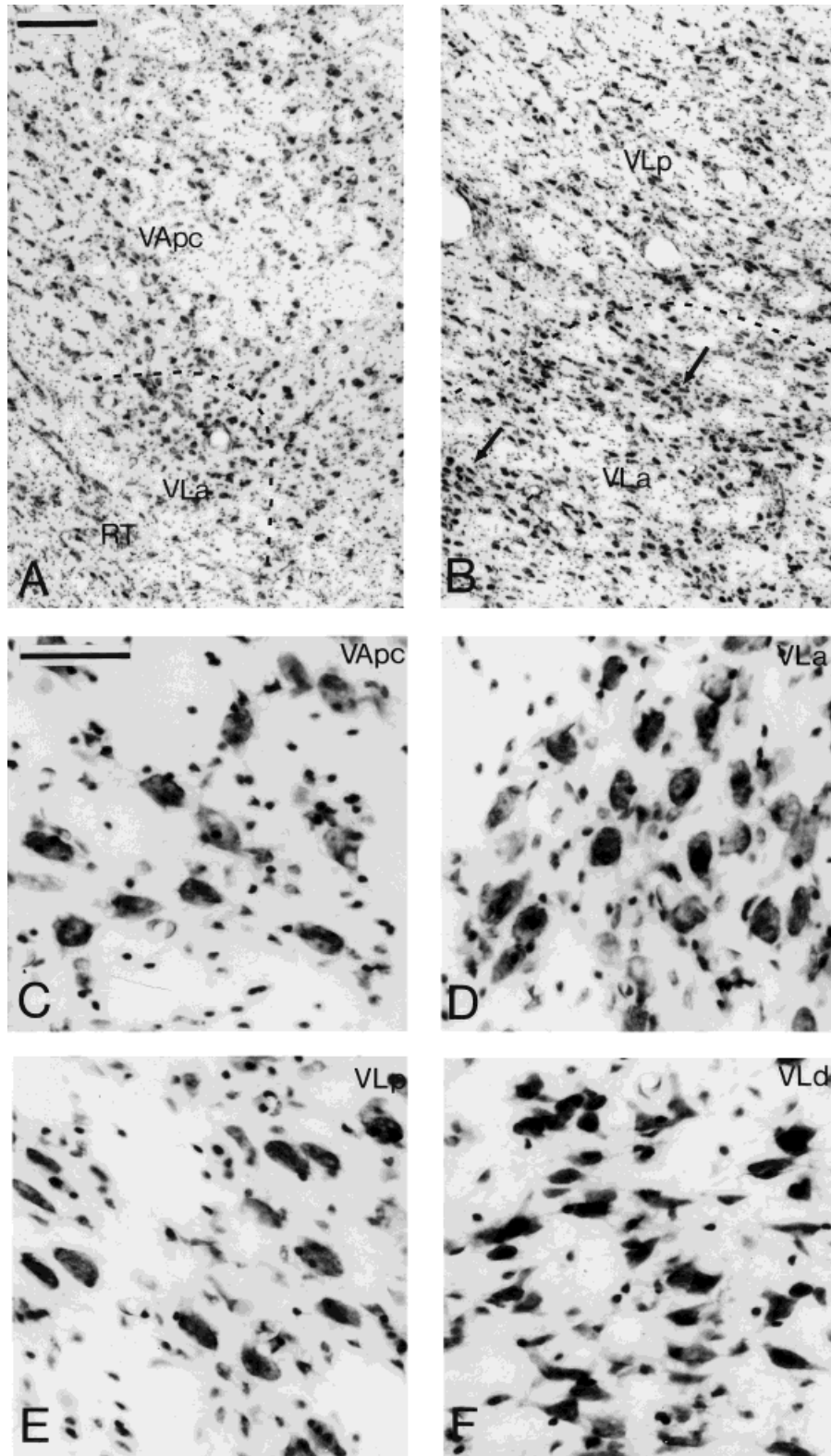


Fig. 2. Nissl-stained subnuclei of the ventrolateral nuclear group showing the cytoarchitectonic features of the component neurons. **A:** The anterior ventrolateral nucleus (VLa) and the parvocellular ventral anterior nucleus (VApc) at a rostrocaudal level corresponding to A10.5. The dashed line indicates the boundary between the two nuclei. Note that VLa neurons are clustered, whereas VApc cells are more sparsely distributed. The size and shape of the neuronal perikarya in these two nuclei are different; VLa cells are smaller and

more ovoid than VApc neurons (C,D). **B:** The VLa and the principal ventrolateral nucleus (VLp) at a level corresponding to A8.5. The dashed line indicates the boundary between the two nuclei. The main feature of the VLp is the large number of axon bundles, among which are scattered a few large-sized neurons. In the VLa, the neurons are much more numerous and form dense clusters (arrows). **C-F:** Examples of neurons in the different subnuclei. Scale bars = 0.5 mm in A (also applies to B), 50 μ m in C (also applies to D-F).

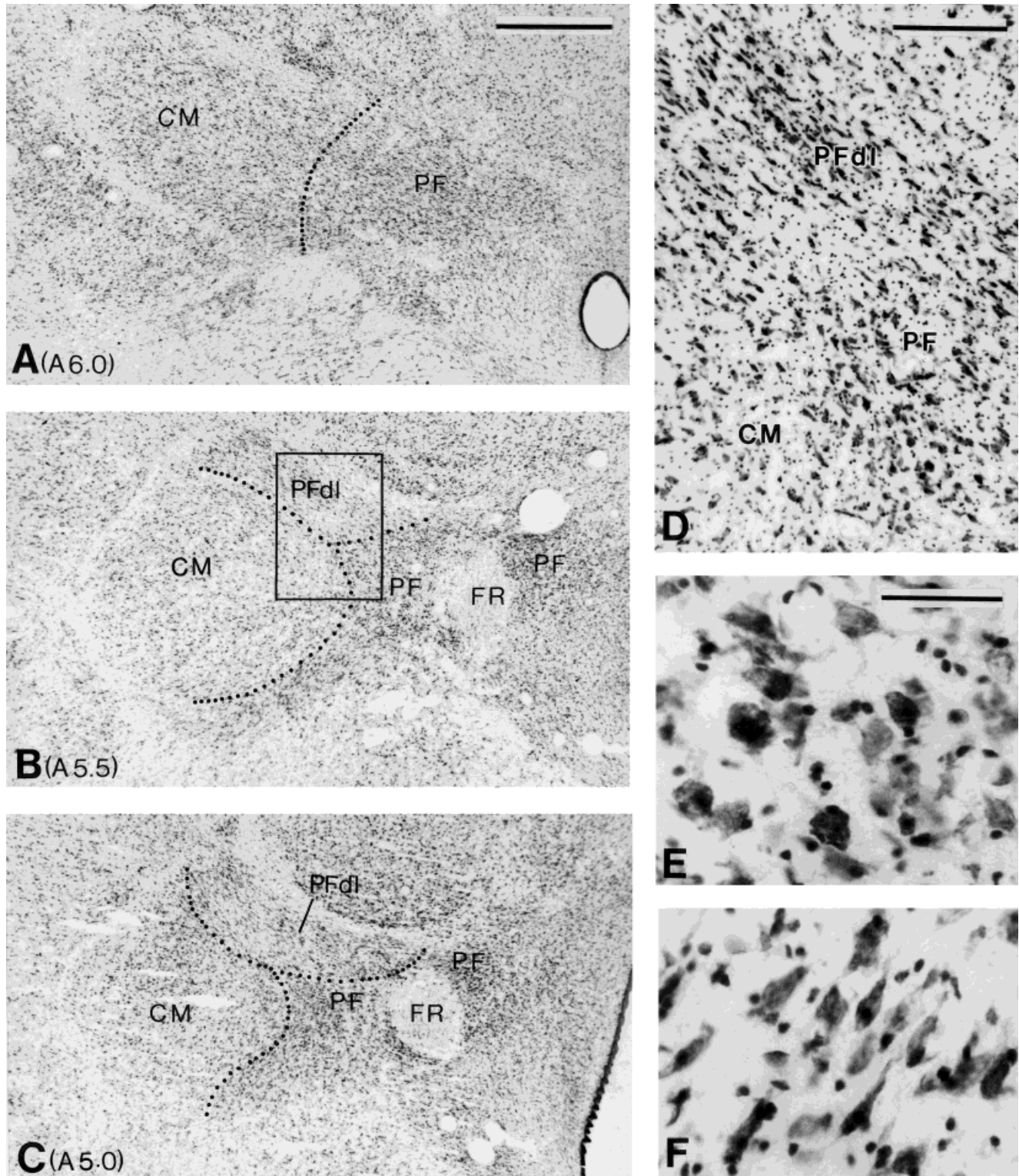


Fig. 3. **A-C:** Nissl-stained transverse sections through the centromedian/parafascicular nuclei (CM/PF) showing the different subdivisions of the nuclear complex at different rostrocaudal levels. The anteroposterior stereotaxic coordinates are indicated in the lower left corner of each micrograph. The dots indicate the limits between the different parts of the nuclear group. The region in the rectangle in B is shown at higher magnification in **D**. Note the difference in cellular

density and morphology between the CM, the PF, and the dorsolateral PF (PFdl). **E:** Examples of neuronal perikarya in the PF. **F:** The morphology of cells in the PFdl. Note the different shape and orientation of the neuronal perikarya in the two subdivisions of the PF. Scale bars = 1.0 mm in A (also applies to B,C), 100 μm in D, 50 μm in E (also applies to F).

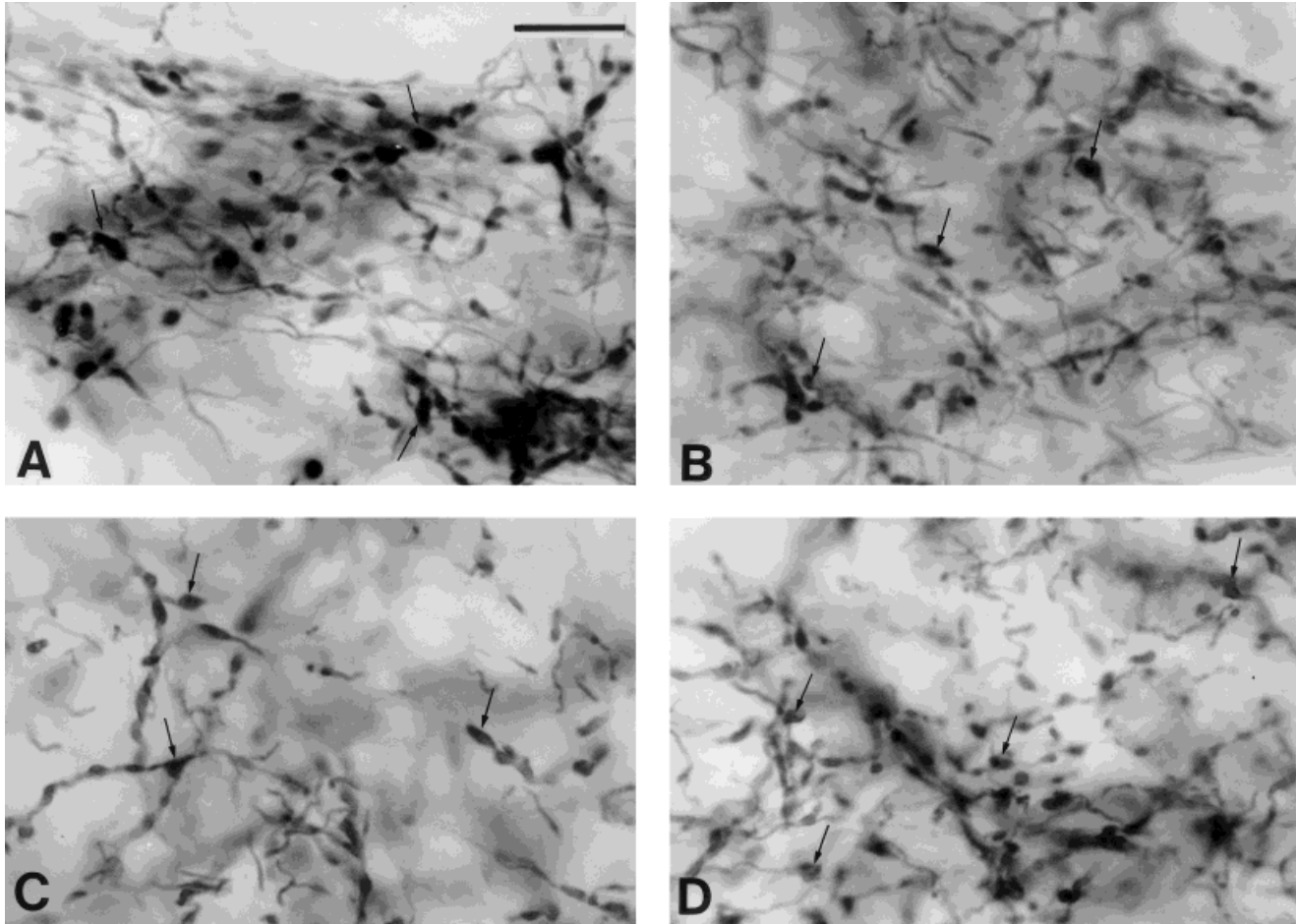


Fig. 4. Light micrographs showing morphological features of biotinylated dextran amine (BDA)-containing varicose fibers in the VLp (A), VApC (B), VLp (C), and dorsal ventrolateral nucleus (VLd; D) after injections of BDA in different regions of the internal pallidum (GPI). The fibers in the VLp, VApC, and VLd were labelled after injections in

the associative territory of the GPI, whereas the fibers in the VLp resulted from an injection in the sensorimotor territory of the GPI. Note that the fibers in the four subnuclei of the VA/VL display common morphological characteristics. The arrows indicate varicosities. Scale bar = 25 μ m.

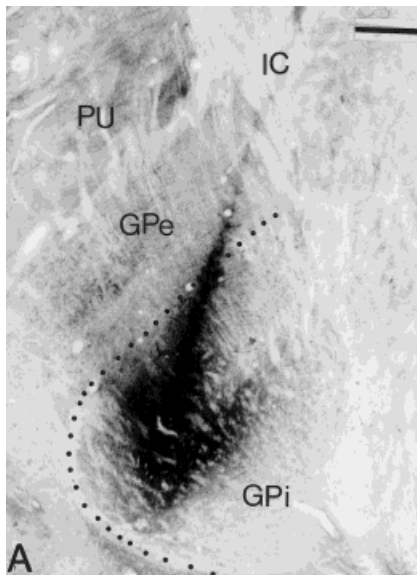
particularly those that arborized in the PFdl, were oriented in the mediolateral direction and did not show any particular association with neuronal perikarya (Fig. 11B,D–G). Many fibers crossed the midline at the level of the rostral pole of the CM to reach the contralateral side.

Distribution of anterogradely labelled fibers in the VA/VL and the CM/PF

Group 1: Injections in the ventrolateral two-thirds of the GPI. In three cases, the BDA injections involved mainly the ventrolateral two-thirds of the central part of the GPI (A9.5–A10.0 in the rostrocaudal plane). The location of the injection site and the resulting anterograde labelling in the thalamus in a typical case of this experimental group are illustrated in Figures 5 and 10A–C. Although the tracer slightly leaked along the injection track, the angle of penetration ensured that it avoided the dorsal part of the GPI (Fig. 5A). The internal capsule was not contaminated by this injection. The rostral pole of the VA/VL was almost completely devoid of anterograde labelling except for scattered varicose fibers in the VLp and the VApC (Fig. 5B,C). The most intensely labelled subnucleus was the rostral part of the VLp (Figs. 5D,E, 9). At this level, a dense band

of anterograde labelling extended throughout the entire dorsoventral extent of the nucleus. This band was made up with dense clusters of labelled varicose fibers separated by zones containing a lower density of labelled elements (Figs. 5D,E, 9). In the mediolateral plane, the band of labelling was located in the central part of the nucleus, leaving an unlabelled region along the reticular nucleus. In other cases of this group, larger injections of BDA that extended more medially in the GPI led to bands of labelling similar to that shown in Figure 5D but with a slight lateral shift in the VLp. The magnocellular part of the VA (VAmc), the caudal part of the VLp, the VLx, and the VLd were devoid of anterogradely labelled structures (Fig. 5B–E).

In the CM/PF, dense anterograde labelling was strictly confined to the CM throughout its entire rostrocaudal extent (Fig. 10A–C). At the level of its middle one-third, the cluster of anterogradely labelled elements was found in the medial part of the nucleus (Fig. 10B), whereas, more caudally, the labelling was shifted laterally (Fig. 10C). The caudolateral one-third of the nucleus remained devoid of labelling (Fig. 10C).



GROUP 1

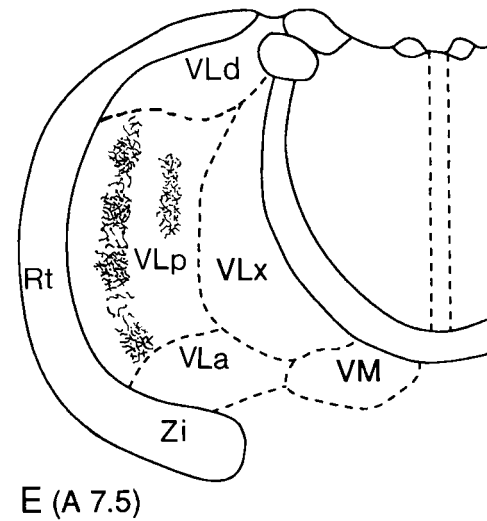
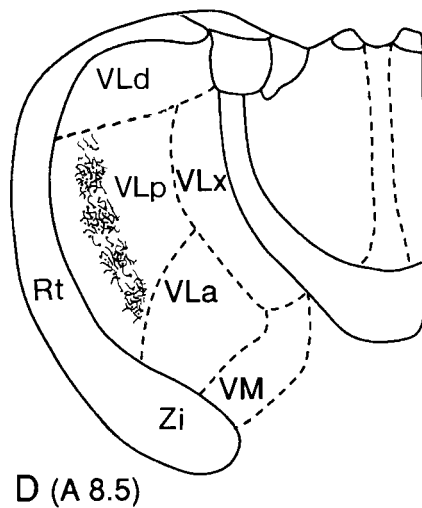
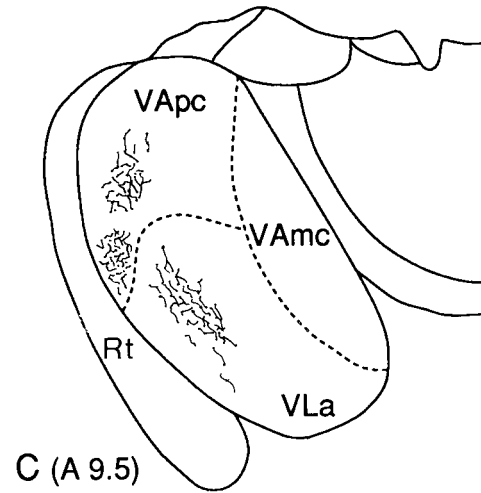
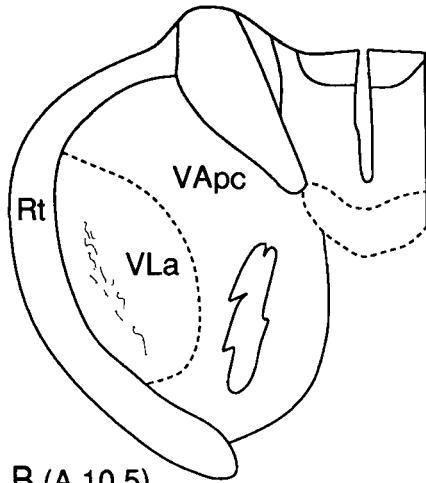
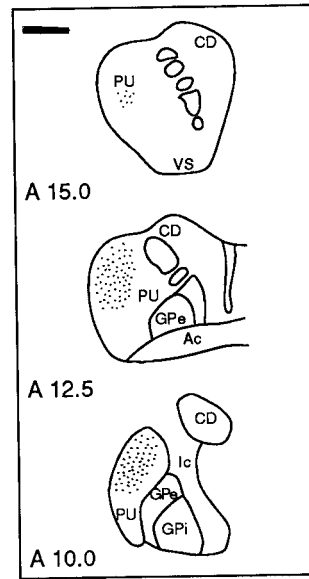
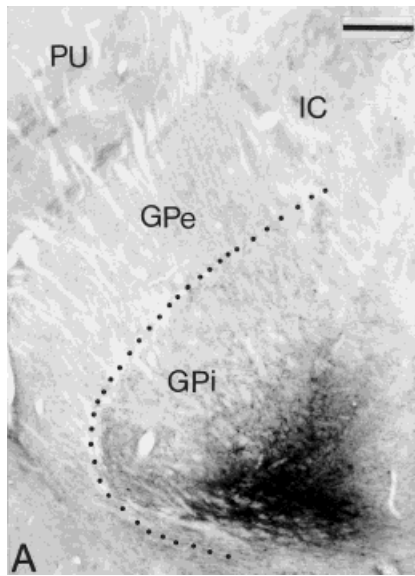
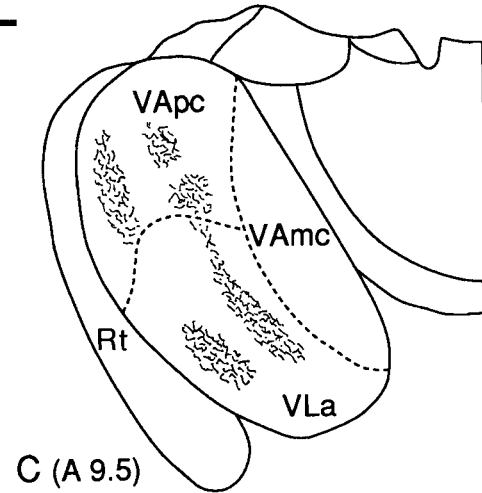
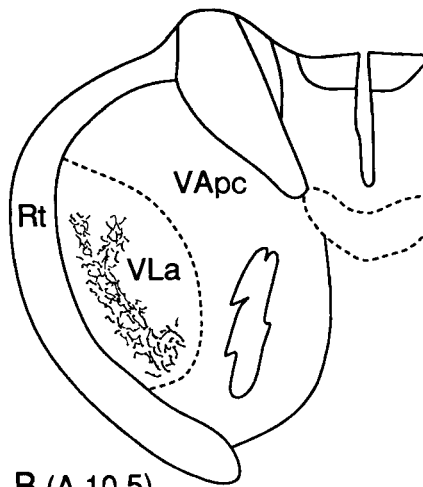
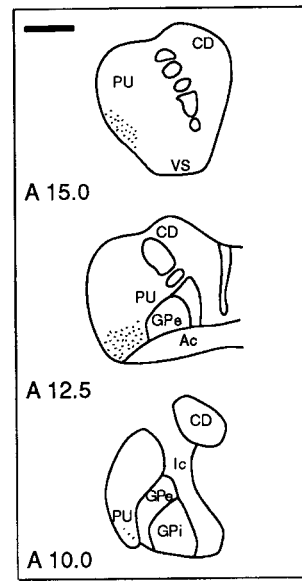


Fig. 5. **A,A'**: Group 1. BDA injection site in the ventrolateral two-thirds of the GPI and resulting retrograde labelling in the striatum. **B-E**: Distribution of anterograde labelling in the VA/VL. The anteroposterior coordinates indicated in the lower left corner of

each section in this and subsequent drawings were determined according to the atlas of Emmers and Akert (1963). For abbreviations, see list. Scale bars = 1.0 mm in A, 2.0 mm in A', 1.0 mm in B-E.

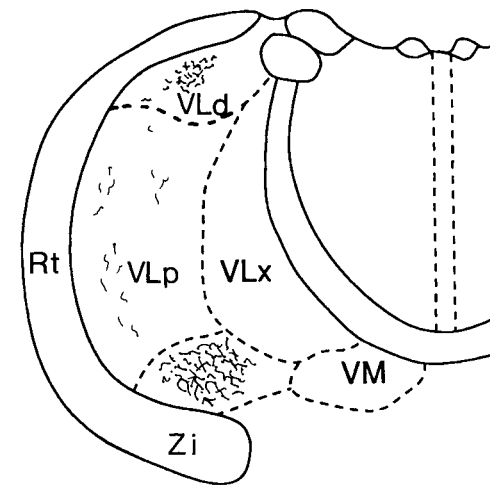
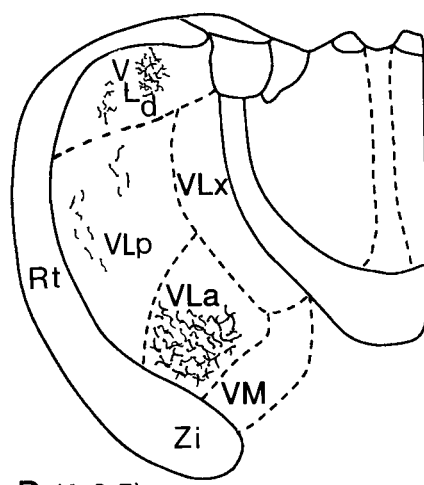


GROUP 2



B (A 10.5)

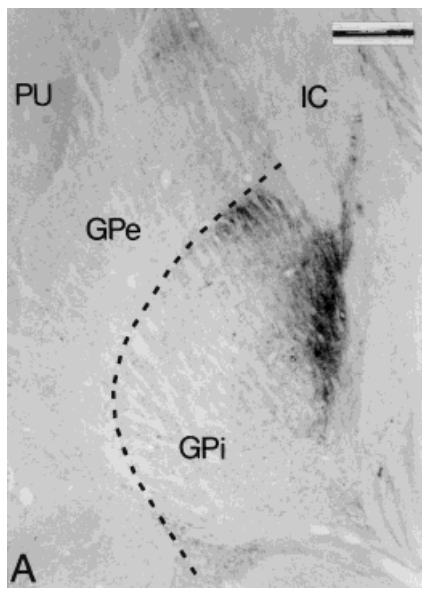
C (A 9.5)



D (A 8.5)

E (A 7.5)

Fig. 6. A,A': Group 2. BDA injection site in the ventromedial part of the GPi and resulting retrograde labelling in the striatum. B-E: Distribution of anterograde labelling in the VA/VL. The anteroposterior coordinates are indicated in the lower left corner of each section. For abbreviations, see list. Scale bars = 1.0 mm in A, 2.0 mm in A', 1.0 mm in B-E.



GROUP 3

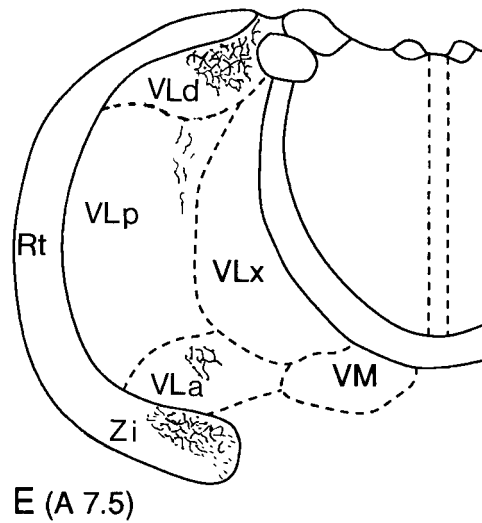
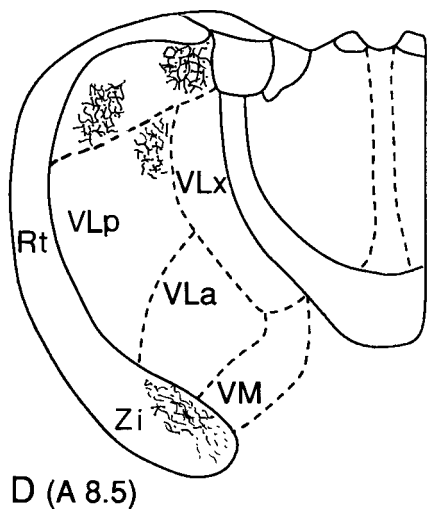
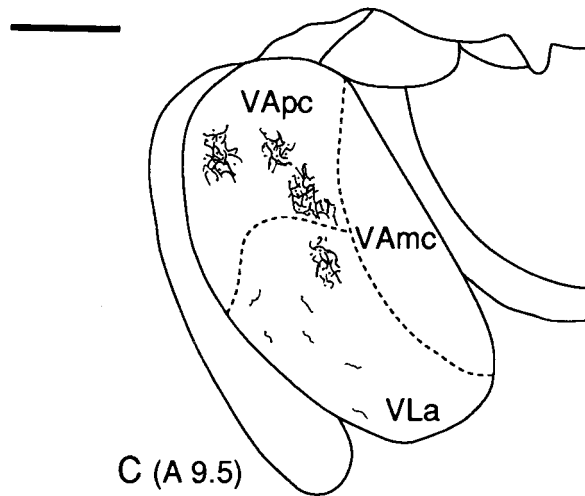
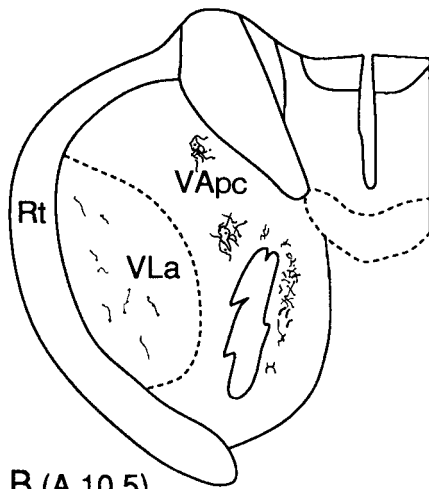
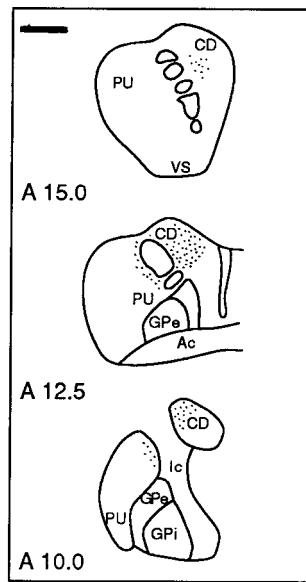
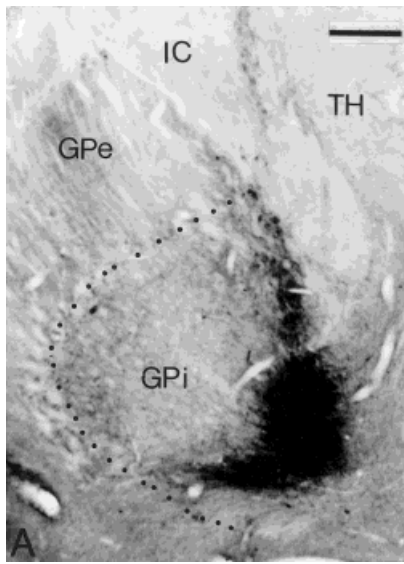


Fig. 7. **A,A'**: Group 3. BDA injection site in the dorsal one-third of the GPi and resulting retrograde labelling in the striatum. **B-E**: Distribution of anterograde labelling in the VA/VL. The anteroposterior coordinates are indicated in the lower left corner of each section. For abbreviations, see list. Scale bars = 1.0 mm in A, 2.0 mm in A', 1.0 mm in B-E.



GROUP 4

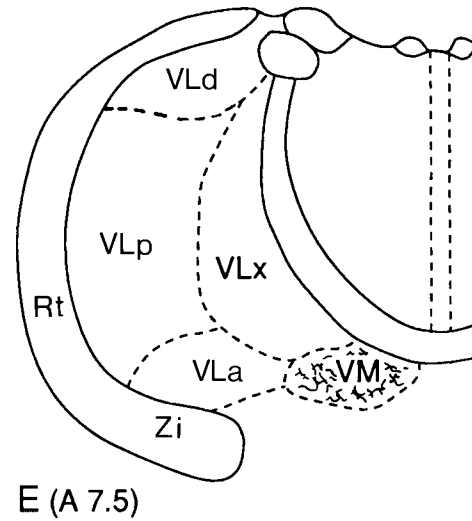
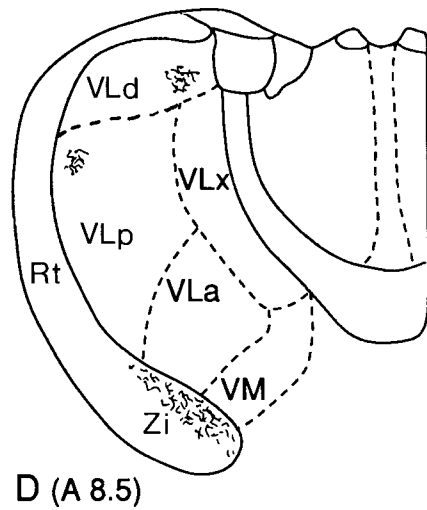
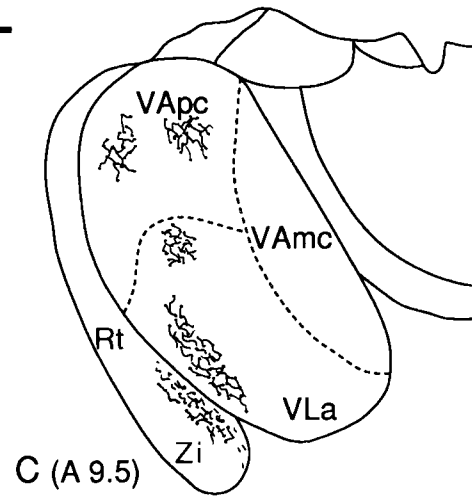
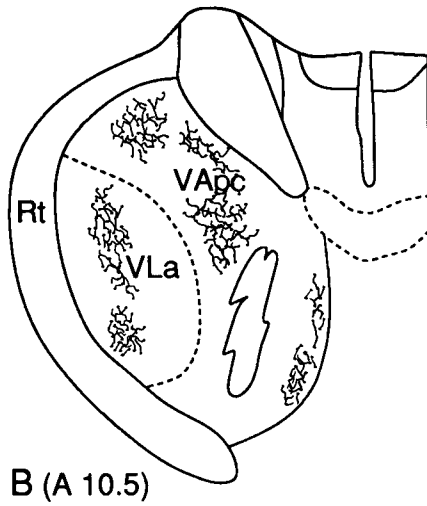
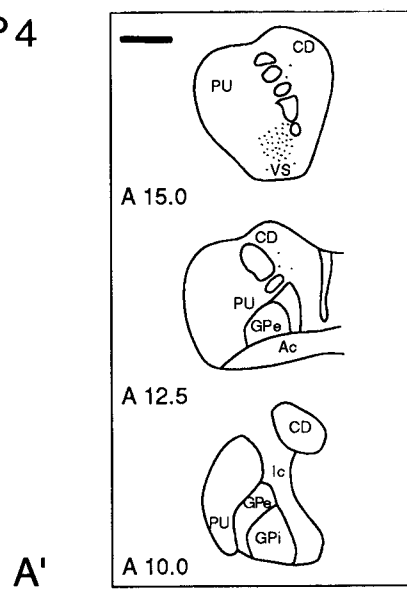


Fig. 8. **A,A'**: Group 4. BDA injection site in the rostromedial pole of the GPi and resulting retrograde labelling in the striatum. **B-E**: Distribution of anterograde labelling in the VA/VL. The anteroposterior coordinates are indicated in the lower left corner of each section. For abbreviations, see list. Scale bars = 1.0 mm in A, 2.0 mm in A', 1.0 mm in B-E.

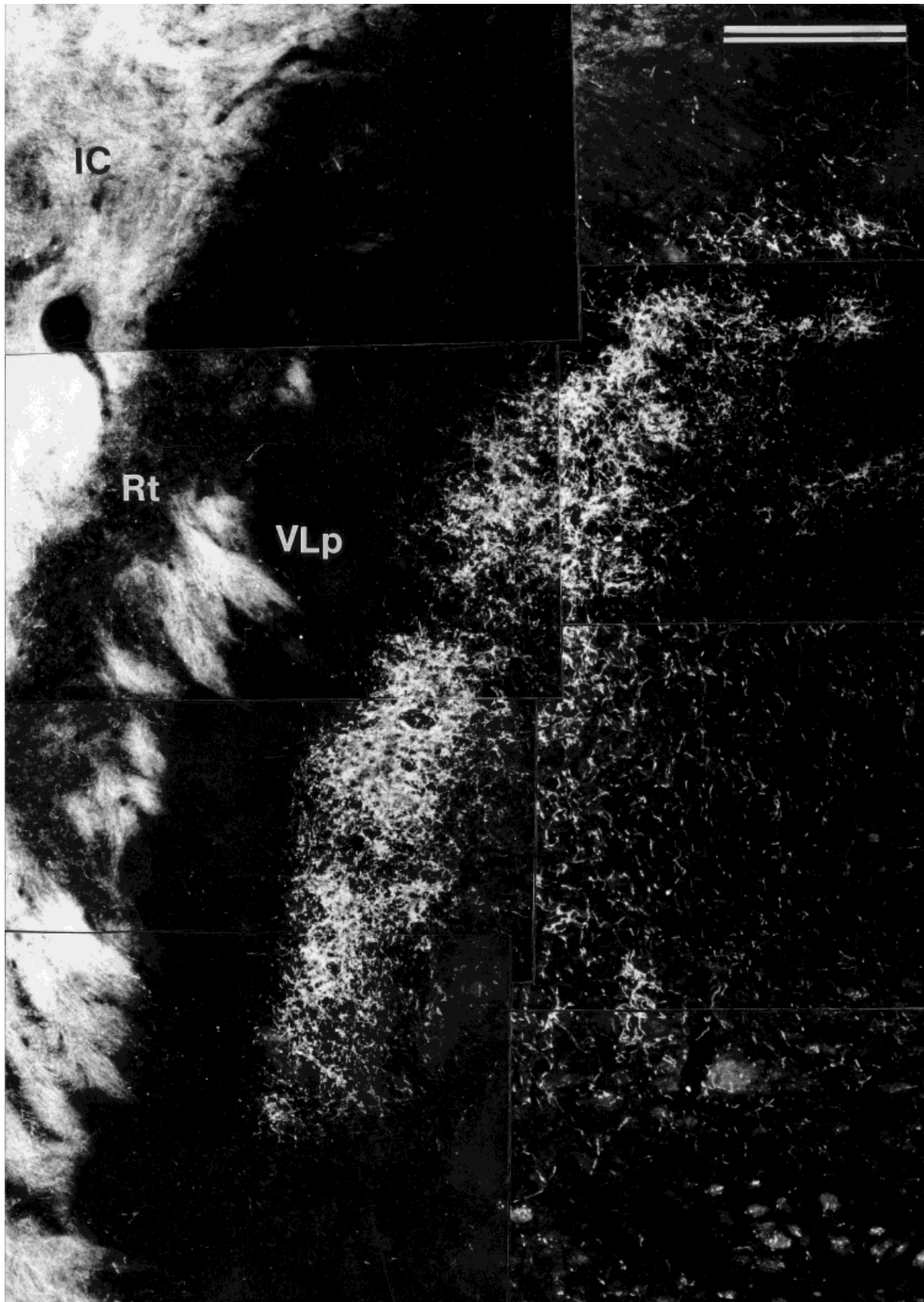


Fig. 9. Darkfield photomicrograph showing a band of anterogradely labelled varicose fibers in the rostral VLp following an injection of BDA in the ventrolateral two-thirds of the GPi (Fig. 5A, group 1). For abbreviations, see list. Scale bar = 0.5 mm.

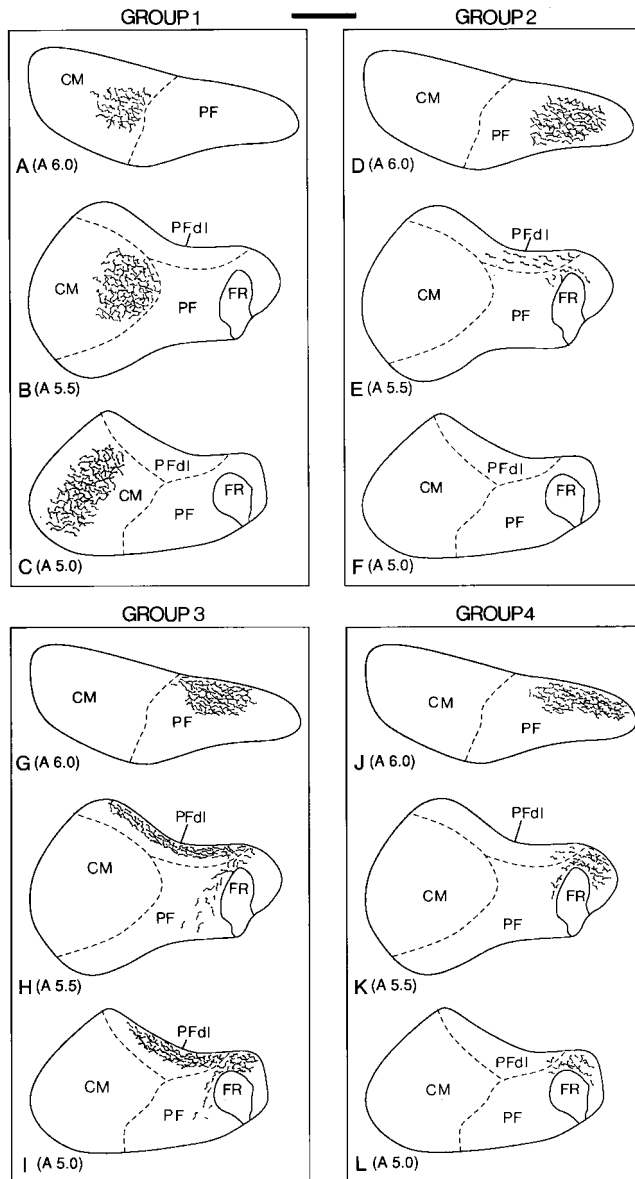


Fig. 10. Schematic drawings of transverse sections through the rostrocaudal extent of the CM/PF nuclear complex illustrating the distribution of anterogradely labelled fibers in experimental groups 1–4. The injection sites for each group are shown in Figures 5A, 6A, 7A, and 8A, respectively. For abbreviations, see list. Scale bar = 0.5 mm.

Group 2: Injections in the ventromedial part of the GPI. In two cases, the injections were located approximately 0.5 mm more rostral and more medial than those in group 1. The injection site and the resulting anterograde labelling in a representative case of this group are shown in Figures 6 and 10D–F. The ventrolateral and dorsal two-thirds of the GPI were largely avoided by these injections (Fig. 6A). The tracer did not leak in the internal capsule or in the cerebral cortex along the injection tracks (Fig. 6A). The VLa was the most intensely labelled subdivision of the VA/VL, although fibers were also found in the VApc and the VLd (Fig. 6C,D). Rostrally, the labelling in the VLa

displayed a band-like pattern (Fig. 6B,C), as was the case for the labelling in VLp in the preceding group.

At the level of the CM/PF, the BDA-containing fibers were largely confined to the rostral one-third of the nuclear complex, where they formed a dense plexus in the central part of the PF (Fig. 10D–F). More caudally, a few fibers oriented in the mediolateral direction lay along the medial part of the PFdl (Fig. 10E). The CM was devoid of labelling throughout its entire extent.

Group 3: Injections in the dorsal one-third of the GPI. In two cases of this group, the injection sites involved the dorsomedial part of the GPI at a rostrocaudal level corresponding to A9.5–A10.0 according to the atlas of Emmers and Akert (1963; Fig. 7A). The location of the injection site and the resulting anterograde labelling in the thalamus in a representative case of this group are illustrated in Figures 7 and 10G–I. The VApc and the VLd (Fig. 7) contained dense clusters of varicose fibers, whereas the VLa and the VLp were almost completely devoid of labelling after these injections (Fig. 7). Anterogradely labelled varicose fibers were also found in the dorsal one-third of the zona incerta (Fig. 7D,E). The morphology of the labelled fibers in the zona incerta was quite similar to that described for those in the VA/VL.

In the rostral one-third of the CM/PF, varicose fibers invaded the dorsolateral part of the PF (Fig. 10G–I), whereas, in the caudal two-thirds of the complex, the labelled fibers formed a dense band that lay along the dorsal half of the PFdl (Figs. 10G–I, 11C,D). At these levels, the PF contained a few fibers that coursed dorsoventrally along the fasciculus retroflexus (Fig. 10H,I). The CM was devoid of labelling throughout its entire extent (Fig. 10G–I).

In another case of this group (not illustrated), the injection site was 0.5 mm more rostral than that in Figure 7A and involved the dorsolateral part of the GPI. The pattern of anterograde labelling in the VA/VL and CM/PF was quite similar to that described above (Fig. 7B–E).

Group 4: Injections in the rostromedial pole of the GPI. In the two cases of this group, the injection sites were quite similar and led to the same pattern of anterograde labelling in the VA/VL and the CM/PF. The location of the injection site and the thalamic labelling in a representative case of this group are shown in Figures 8 and 10K–M. The most intensely labelled nucleus was the rostral part of the VApc, whereas moderate labelling was found in the rostral pole of the VLa and the VM. It is worth noting that only these injections led to anterograde labelling in the VM. All the other subnuclei of the VA/VL were almost completely devoid of anterograde labelling (Fig. 8B–E). Like the case in group 3, anterograde labelling occurred in the dorsal part of the zona incerta (Fig. 7C,D).

At the level of the CM/PF, the anterograde labelling was confined to the dorsal part of the rostral two-thirds of the PF (Fig. 10K–M). The CM and the PFdl were not labelled in these cases.

Electron microscopic observations

All of the electron microscopic observations were made in the case illustrated in Figure 5. Six blocks were taken from regions of the VLp and CM that were enriched in BDA-positive terminals. In the electron microscope, the BDA-positive structures were recognized by the presence of a dense, amorphous reaction product. In both the VLp and the CM, the BDA-labelled elements included myelin-

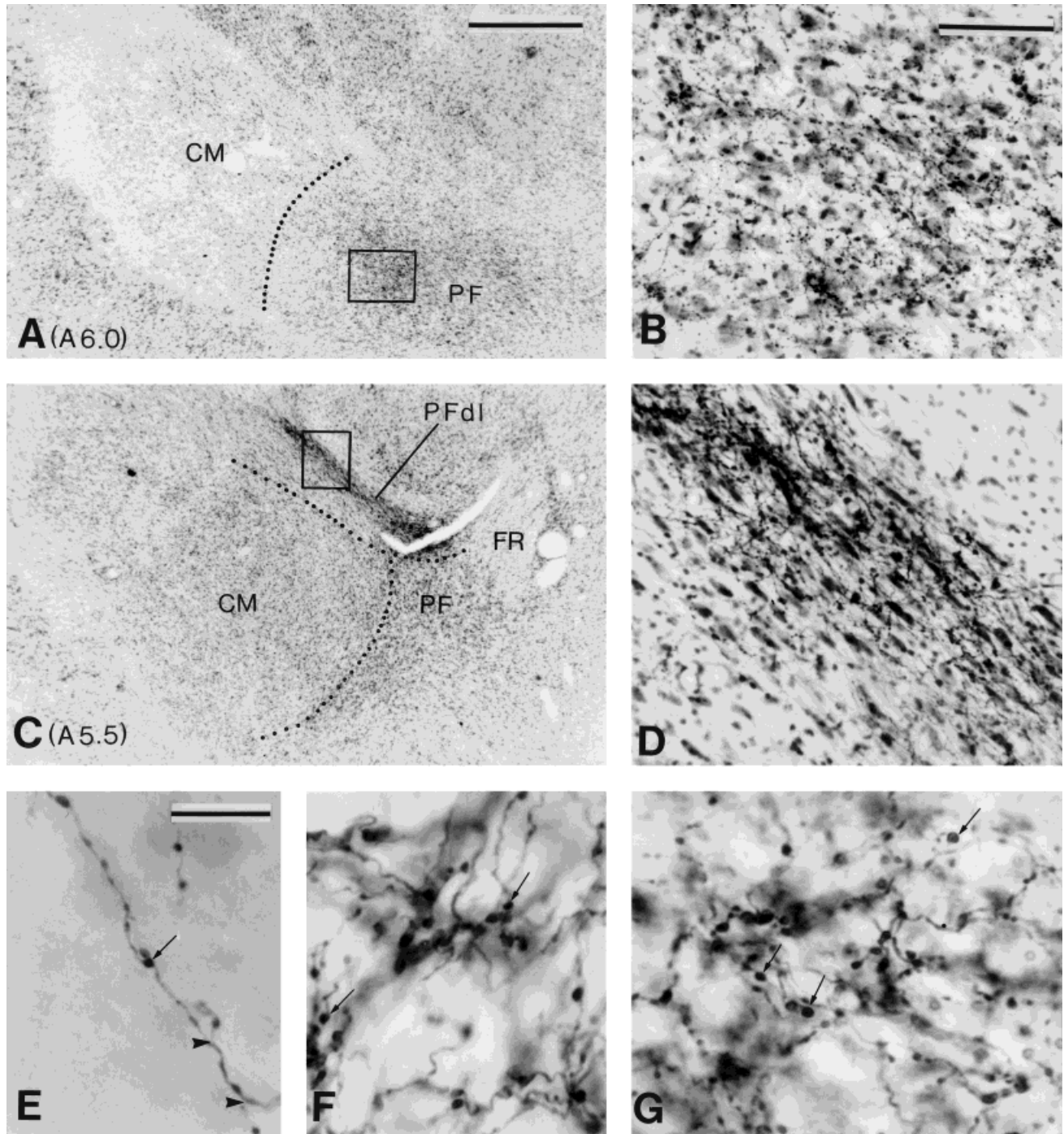


Fig. 11. **A-G:** Photomicrographs showing BDA-labelled terminals in the CM/PF nuclear complex after injections of BDA in the rostromedial pole (group 4; A,B,E), the dorsal one-third (group 3; C,D,F), and the ventrolateral two-thirds (group 1; G) of the GPi. The sections in A and C have been counterstained with thionin to delineate the limit between the different subnuclei. A shows a low-power view of an aggregate of labelling in the PF of group 4. The dotted lines indicate the limit between the CM and the PF. The area in the rectangle is shown at higher magnification in B. C illustrates a band of labelling in

the PFDl of group 3. The area in the rectangle is shown at higher magnification in D. In A and C, the anteroposterior stereotaxic coordinates are indicated. E shows a varicose fiber from which emerge axon collaterals (arrowheads) in the PF of group 4. Note that this fiber bears varicosities of different sizes (arrow). F shows varicose fibers (arrows) in the PFDl of group 3. G illustrates labelled varicose fibers (arrows) in the CM of group 1. For abbreviations, see list. Scale bars = 1 mm in A (also applies to C), 100 μ m in B (also applies to D), 25 μ m in E (also applies to F,G).

ated and unmyelinated axons (Fig. 12A) as well as terminal boutons (Fig. 12B–D).

In the VLp, the BDA-positive boutons displayed common ultrastructural features. They were large (maximum diameter ranging from 1.5 μm to 5.0 μm), contained many mitochondria, and were packed with pleomorphic, electron-lucent vesicles (Fig. 12). Occasionally, one or two dense core vesicles were encountered. These boutons often had an elongated shape and formed symmetric synapses with short active zones (Fig. 12C). In about 10% of the cases, the symmetric membrane specialization was difficult to ascertain because of dense reaction product that obscured the synaptic vesicles in the presynaptic elements (Fig. 12D). However, none of the contacts established by those darkly labelled boutons was associated with postsynaptic densities, which indicates that the synapses were not of the asymmetric type. Because they displayed ultrastructural features that resembled those of labelled terminals forming symmetric synapses, we assumed that they arose from the GPi. Among the 207 labelled boutons examined, 47.3% formed synapses with large dendrites (diameter $>$ 1.0 μm ; Fig. 14). The remaining terminals were in contact with medium-sized (diameter between 0.5 μm and 1.0 μm ; 22.7%; Figs. 12C,D, 14) or small (diameter $<$ 0.5 μm ; 23.6%; Figs. 12C, 14) dendrites and with perikarya (5.7%; Figs. 12B, 14). A single terminal (0.4%) formed a synapse with a spine. The dendrites contacted by the GPi terminals frequently received asymmetric synaptic inputs from small unlabelled boutons packed with round synaptic vesicles. More than 95% of the postsynaptic dendrites with a well-preserved ultrastructure did not contain synaptic vesicles (Fig. 12C,D), an indication that they belong to relay cells (Jones, 1985).

In the CM, the majority of BDA-containing boutons also contained numerous mitochondria and pleomorphic vesicles but were smaller than those in the VLp (maximum diameter ranging between 0.5 μm and 1.5 μm ; Fig. 13A–D). In some cases, the boutons were too darkly stained to ascertain the type of synaptic junctions. Such terminals were not considered for the characterization of postsynaptic targets to pallidal boutons in the CM (Fig. 14). In general, pallido-CM terminals had an ovoid shape and formed symmetric synapses predominantly with large (38.8%; $n = 33$) and medium-sized (30.5%; $n = 26$) dendrites (Figs. 13A,B, 14) and, much less frequently, with small dendrites (15.2%; $n = 13$; Figs. 13C, 14), spines (8.2%; $n = 7$) and perikarya (7.0%; $n = 6$; Figs. 13D, 14). Some of the dendrites contacted by BDA-positive terminals, as was the case in the VLp, also received asymmetric synaptic input from small boutons packed with round, electron-lucent vesicles (Fig. 13C). Another rare type ($n = 5$) of BDA-positive boutons that was encountered in the CM contained round synaptic vesicles and formed asymmetric synapses with medium-sized dendritic shafts (Fig. 13E). Some of these terminals contacted two dendrites, which, in some cases, contained synaptic vesicles (Fig. 13E).

DISCUSSION

The use of the retrograde-anterograde tracer BDA allowed us to trace the efferent projections of regions of the GPi that receive inputs from different functional territories of the striatum. Three major conclusions can be drawn from our findings. First, projections from the sensorimotor territory of the GPi, i.e., the ventrolateral two-thirds of the

structure, are largely segregated from those arising from the associative and limbic territories at the level of the ventrolateral thalamus. In contrast, projections arising from the associative and limbic GPi appear to innervate common subnuclei of the VA/VL (Fig. 15 A–E). Second, our findings clearly indicate that the pallidal inputs to the CM/PF are segregated according to their origin in the GPi. The sensorimotor GPi projects to the CM, whereas the associative and limbic GPi innervate the PF and the PFdl (Fig. 15F). Third, the GPi terminals innervate preferentially the proximal dendrites of relay neurons in the VLp and the CM.

Convergence of pallidal inputs to the VA/VL

One of the new findings of the present study is that projections arising from regions of the GPi that receive afferents from different populations of striatal neurons either remain largely segregated in different subnuclei or converge to common regions in the VA/VL. For instance, the ventrolateral two-thirds of the GPi, which receive afferents from the sensorimotor territory of the striatum, project to the VLp, whereas projections arising from other regions of the GPi avoid this subnucleus. On the other hand, the dorsal one-third and rostromedial pole of the GPi, which receive inputs from the caudate nucleus and the ventral striatum, respectively, appear to innervate common regions in the VApC and the VLd. The functional implication of this segregation and convergence of pallidal inputs at the thalamic level largely relies upon the origin of cortical inputs to striatopallidal neurons that innervate those regions of the GPi that received injections of BDA. For instance, if neurons in the ventral striatum and neurons in the caudate nucleus receive cortical inputs from segregated functional areas of the cerebral cortex, then the convergence of pallidothalamic projections disclosed in our study provides a substrate by which parallel corticostriatopallidal pathways cross-talk at the thalamic level. On the other hand, if the segregation of cortical inputs to retrogradely labelled neurons in the ventral striatum and the caudate nucleus is not absolute, then the fact that their pallidal outputs converge at the thalamic level indicate that these regions cross-talk at different levels through the basal ganglia-thalamocortical circuitry. On the basis of extensive tract-tracing studies carried out in macaques, the cortical inputs to the part of the caudate nucleus that contained retrogradely labelled cells after BDA injection in the dorsal one-third of the GPi arise preferentially from the dorsolateral and dorsomedial prefrontal cortex, the posterior parietal cortex, and the frontal eye field (Künzle and Akert, 1977; Yeterian and Van Hoesen, 1978; Selemon and Goldman-Rakic, 1985; Stanton et al., 1988; Yeterian and Pandya, 1991, 1993). On the other hand, the region of the ventral striatum labelled after BDA injections in the rostromedial pole of the GPi receives inputs from limbic-related cortices, such as the temporal polar region (Yeterian and Van Hoesen, 1978; Van Hoesen et al., 1981; Selemon and Goldman-Rakic, 1985; Yeterian and Pandya, 1991; Haber et al., 1995), the cingulate cortex, the orbitofrontal cortex (Yeterian and Van Hoesen, 1978; Selemon and Goldman-Rakic, 1985; Yeterian and Pandya, 1991; Kunishio and Haber, 1994; Haber et al., 1995), and the amygdala (Russchen et al., 1985). The results of our study therefore imply that associative and limbic cortical information, which remains segregated at the level of the striatopallidal complex, is

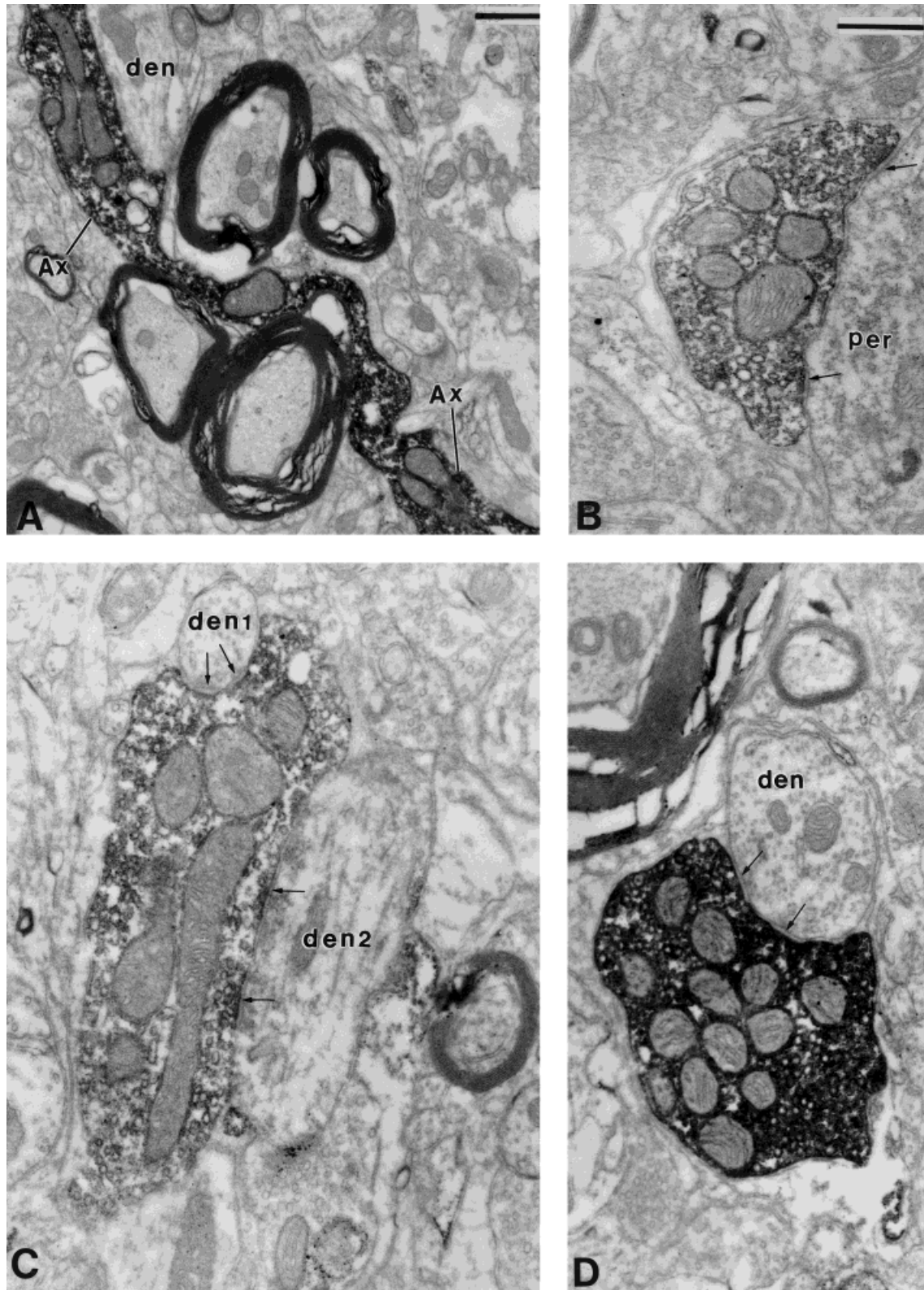


Fig. 12. Electron micrographs showing ultrastructural features of a BDA-positive axon (A) and anterogradely labelled terminals (B-D) in the VLP after injection in the ventrolateral two-thirds of the GPI (group 1). A shows an unmyelinated axon (Ax) that gives rise to a terminal bouton apposed on the surface of a dendritic shaft (den). B-D show BDA-positive boutons that form symmetric synapses (indicated by arrows) with small (C, den1) and medium-sized (C,D, den2)

dendrites. B shows a bouton in symmetric contact with a perikaryon (per). In some boutons, the 3,3'-diaminobenzidine tetrahydrochloride (DAB) staining is so strong that it obscures the synaptic vesicles in the presynaptic elements (D). This was a problem for about 10% of the labelled boutons examined in the VLP. For other abbreviations, see list. Scale bars = 1.0 μ m in A, 0.5 μ m in B (also applies to C,D).

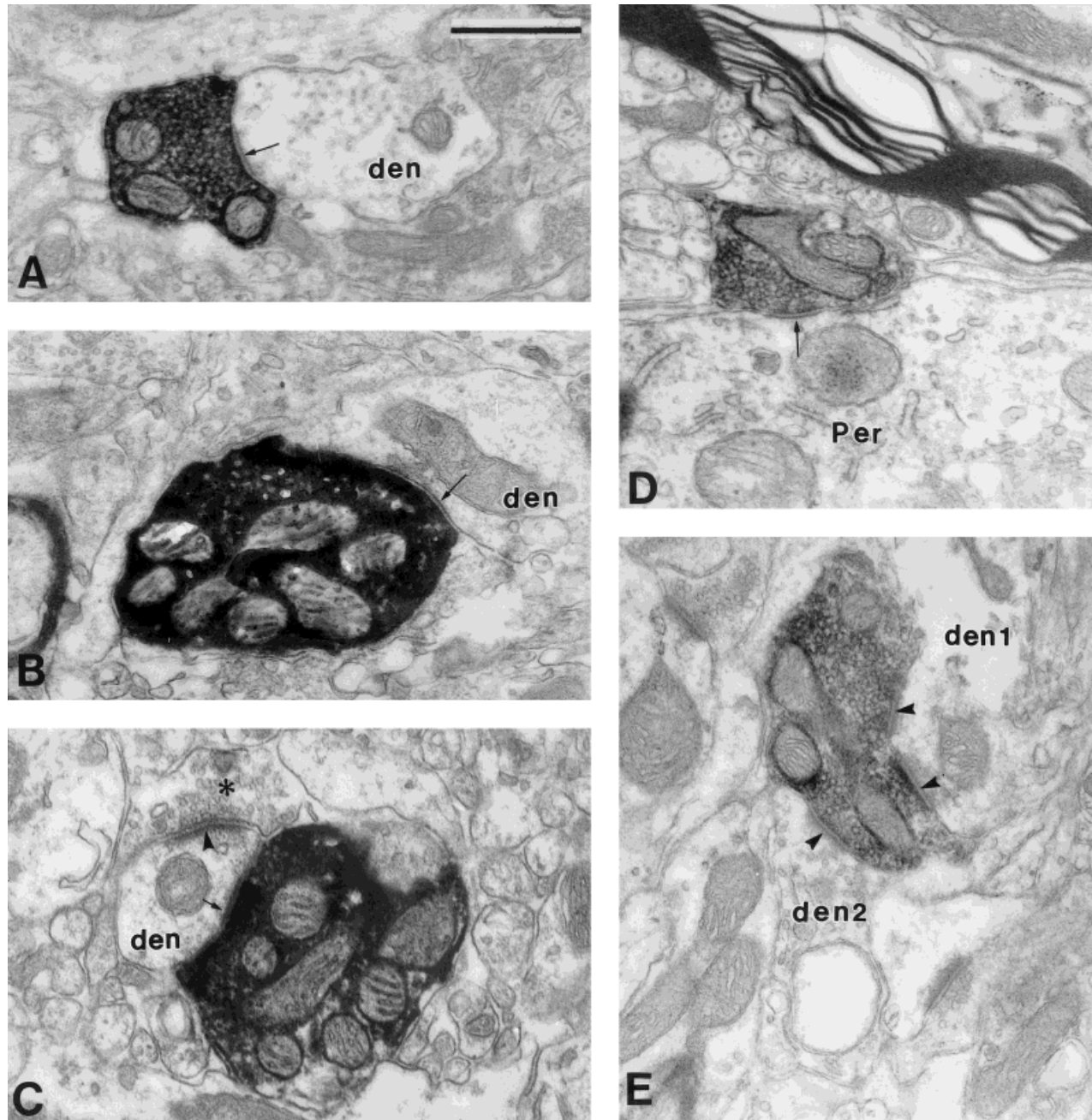


Fig. 13. Electron micrographs showing examples of anterogradely labelled boutons in the CM after an injection of BDA in the ventrolateral two-thirds of the GPi (group 1). The boutons in A–C form symmetric synapses (arrows) with dendritic shafts (den), whereas the bouton in D establishes a symmetric synapse with a perikaryon (Per). Note that the dendrite in C also receives an asymmetric synaptic input

(arrowhead) from an unlabelled bouton (asterisk). E illustrates one of the rare BDA-positive boutons that contained round synaptic vesicles and formed asymmetric synapses (arrowheads) with two dendrites (den1 and den2). One of the dendrites (den2) contains synaptic vesicles. Scale bar = 1.0 μ m.

conveyed to common regions of the thalamus. On the other hand, because our observations were made in different cases, we cannot ascertain that limbic and associative GPi outputs converge to individual thalamocortical neurons. Double anterograde labelling studies at the electron microscopic level (Smith and Bolam, 1991, 1992; Smith, 1993) are currently in progress to verify this possibility.

Distribution of sensorimotor-related afferents from the GPi in the VA/VL

In keeping with previous studies (Nauta and Mehler, 1966; Kuo and Carpenter, 1973; Kim et al., 1976; DeVito and Anderson, 1982; Parent and De Bellefeuille, 1982, 1983; Ilinsky and Kultas-Ilinsky, 1987; François et al.,

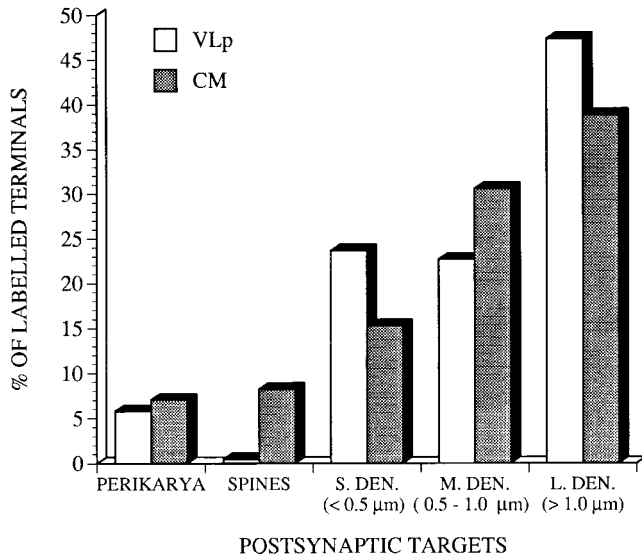


Fig. 14. Histogram showing the relative distribution of the postsynaptic targets contacted by anterogradely labelled GPI terminals in the VLP ($n = 207$) and the CM ($n = 85$). The five terminals that formed asymmetric synapses in the CM were not included in this histogram. S. DEN., small dendrites; M. DEN., medium dendrites; L. DEN., large dendrites.

1988; Fénelon et al., 1990; Hazrati and Parent, 1991; Page et al., 1993; Rouiller et al., 1994; Sakai et al., 1996), injections of BDA in the ventrolateral two-thirds of the GPI resulted in retrograde labelling in the sensorimotor territory of the striatum and led to dense anterograde labelling in the sector of the VA/VL known as the source of projections to motor and supplementary motor cortical areas (Kievit and Kuypers, 1977; Jürgens, 1984; Schell and Strick, 1984; Strick, 1985; Wiesendanger and Wiesendanger, 1985; Leichnetz, 1986; Gosh et al., 1987; Ilinsky and Kultas-Ilinsky, 1987; Matelli et al., 1989; Darian-Smith et al., 1990; Holsapple et al., 1991; Zemanick et al., 1991; Tokuno et al., 1992; Nakano et al., 1993; Tokuno and Tanji, 1993; Stepniewska et al., 1994b; Inase and Tanji, 1995; Shindo et al., 1995). A particular feature that characterized the VLP was the band-like pattern displayed by the pallidal terminals. In line with this pattern of distribution, recent physiological data showed that body parts were represented in a series of parallel lamellae that covered the entire mediolateral extent of the VLo in macaque monkeys (Vitek et al., 1994). Furthermore, retrograde transport studies showed that thalamic neurons projecting to specific areas of the supplementary motor area (SMA) or the primary motor cortex (M1) also display a band-like pattern similar to that observed for the pallidal efferents (Matelli et al., 1989; Darian-Smith et al., 1990; Tokuno and Tanji, 1993; Stepniewska et al., 1994b; Inase and Tanji, 1995; Shindo et al., 1995). On the basis of these physiological and anatomical data, the leg area is represented in the outermost lamella, whereas the trunk, arm, and orofacial regions are represented successively in deeper lamellae. According to this somatotopic organization, the band of labelling shown in Figure 5D,E of our study would fit in the arm-related region. Although the regions of the GPI that were injected have not been physiologically characterized, the correspondence between the location of

our injection site and the relative position of movement-related cells in the GPI of macaques (DeLong and Georgopoulos, 1981; DeLong et al., 1985) suggests that our injections were, indeed, largely confined to the arm-related region of the GPI. Similarly, the injection of BDA in the ventromedial part of the GPI (group 2; Fig. 6) led to anterograde labelling in the caudal part of the VLA, a region of the VA/VL that projects to the face area of M1 (Stepniewska et al., 1994b). This injection site, as expected, partially involved the orofacial-related region of the GPI (DeLong et al., 1985). Moreover, the retrograde labelling generated in the striatum by this injection was located in a region where neurons respond to orofacial movements and evoke discrete movements of the face when stimulated (Alexander and DeLong, 1985). Therefore, it appears that functionally related regions in the GPI and the ventrolateral nuclear group are connected in a highly specific manner in squirrel monkeys. These observations are in line with the concept of parallel processing, which implies that the sensorimotor information relating to specific body parts remains largely segregated in parallel channels that flow through the basal ganglia-thalamocortical circuitry (Alexander et al., 1986; Alexander and Crutcher, 1990).

Cortical projections of VA/VL neurons that receive pallidal inputs

Although it has long been thought that the sensorimotor information from the GPI was conveyed exclusively to the SMA (Schell and Strick, 1984; Strick, 1985; Ilinsky and Kultas-Ilinsky, 1987), recent anatomical and physiological data in macaques demonstrate that the information from the GPI may also be sent to M1. For instance, terminals from the GPI and thalamic cells that project to M1 overlap in the thalamus (Rouiller et al., 1994; Inase and Tanji, 1995). These data were recently extended at the electron microscopic level, showing synaptic contacts between GPI terminals and thalamocortical neurons projecting to M1 (Kayahara and Nakano, 1996). In line with these findings, Hoover and Strick (1993) found retrogradely labelled cells in the VLo and the GPI after injections of herpes simplex virus in the arm area of the primary motor and premotor (PM) cortices. These anatomical data are supported by physiological observations showing that stimulation of the GPI induces inhibitory effects in thalamocortical neurons that were antidromically identified to project to M1 (Nambu et al., 1988, 1991; Jinnai et al., 1993). It is therefore likely that the labelled terminals in the VLP visualized in our study form synapses with thalamocortical neurons that project not only to the SMA but also to M1 and PM in squirrel monkeys. What remains to be established is whether information arising from single pallidal neurons is conveyed to multiple motor cortical areas. This issue is difficult to investigate, because thalamic neurons that project to the SMA and M1 partially overlap (Shindo et al., 1995). Care should thus be taken in the interpretation of light microscopic observations showing overlap between GPI terminals and retrogradely labelled cells from the SMA (Tokuno et al., 1992; Inase and Tanji, 1994; Rouiller et al., 1994) or M1 (Rouiller et al., 1994; Inase and Tanji, 1995). Electron microscopic studies with injections of retrograde tracers in functionally characterized regions of the SMA, M1, and PM combined with injections of anterograde tracers in different regions of the sensorimotor GPI must be carried out for elucidating this issue.

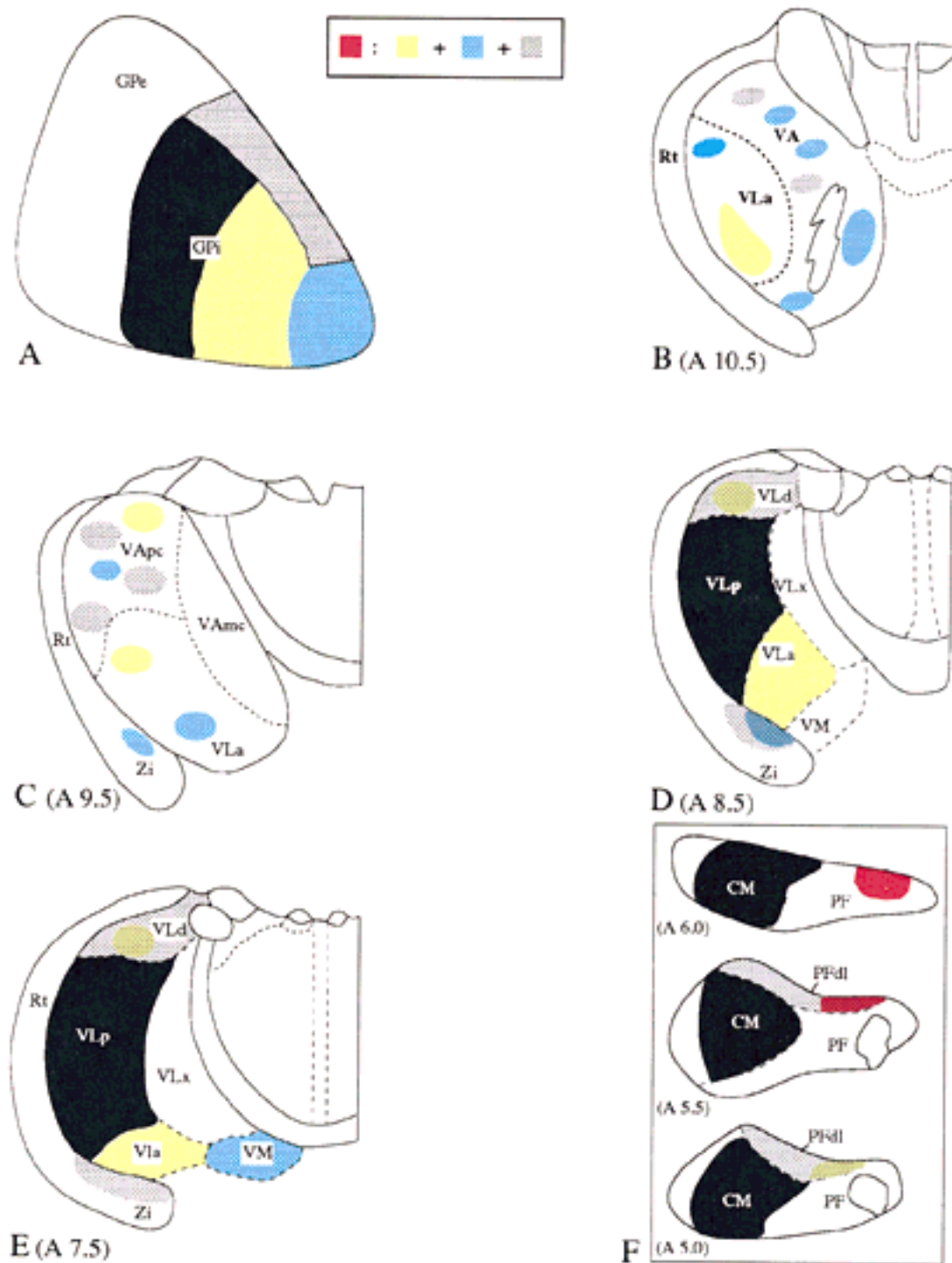


Fig. 15. **A-F**: Schematic diagrams that summarize the pattern of distribution of anterograde labelling through the rostrocaudal extent of the VA/VL (B-E) and the CM/PF (F) after BDA injections in different regions of the GPi in squirrel monkeys (A). The anteroposterior coordinates of each transverse sections of the thalamus are indicated in parentheses. In A, the colored areas in the GPi grossly correspond to the location of the BDA injection sites in the four experimental groups of our study: group 1 (ventrolateral two-thirds of the GPi; black), group 2 (ventromedial part of the GPi; yellow), group 3 (dorsal one-third of the GPi; gray), and group 4 (rostromedial pole of the GPi; blue). For simplification, the injection sites are depicted as though they were all at the same anteroposterior level of the GPi. The areas labelled red in the PF and PFdl (F) correspond to overlapping zones of fibers arising from different parts of the GPi, except for the ventrolateral two-thirds.

In the VApC and the VL_a, the termination fields are shown as occupying nonoverlapping areas, but this must be ascertained by double anterograde labelling studies. We assume that the VL_p is completely filled with terminals from the ventrolateral two-thirds of the GPi (D,E), although a single band of labelling is shown in the case that represents this experimental group (Fig. 5). However, analysis of the distribution of labelling in other cases of this group (not illustrated), which received injections in different parts of the ventrolateral GPi, revealed that the mediolateral position of the band of anterograde labelling in the VL_p varies with the location of the BDA injections in the rostrocaudal plane of the GPi. We therefore assume that a BDA injection filling completely the ventrolateral two-thirds of the GPi would label homogeneously the VL_p. For other abbreviations, see list.

Although the VApC is currently seen as the major target of the dorsal one-third of the GPi (Nauta and Mehler, 1966; Kuo and Carpenter, 1973; Kim et al., 1976; DeVito and Anderson, 1982; Ilinsky and Kultas-Ilinsky, 1987), such is not the case for the VLd. The results obtained in previous anterograde degeneration and tract-tracing studies are indeed controversial regarding the existence of a GPi-VLd projection in primates (Nauta and Mehler, 1966; Kuo and Carpenter, 1973; Kim et al., 1976; DeVito and Anderson, 1982; Ilinsky and Kultas-Ilinsky, 1987; Inase and Tanji, 1994, 1995; Rouiller et al., 1994). Our findings not only demonstrate that the VLd receives GPi afferents, but they also show that this input arises mainly from the associative territory in squirrel monkeys. In addition to the VApC, the VLd may therefore be another major relay whereby the information from the associative territory of the GPi reaches the cerebral cortex. According to previous retrograde tracing studies, neurons in the VLd project to the SMA (Goldman-Rakic and Porrino, 1985; Wiesendanger and Wiesendanger, 1985; Darian-Smith et al., 1990; Inase and Tanji, 1994; Shindo et al., 1995) and M1 (Goldman-Rakic and Porrino, 1985; Darian-Smith et al., 1990; Inase and Tanji, 1995; Shindo et al., 1995) in macaques. The cognitive information from the GPi may therefore be transmitted to prefrontal cortical areas via the VApC (Kievit and Kuypers, 1977; Goldman-Rakic and Porrino, 1985; Middleton and Strick, 1994) and to motor and supplementary motor regions via the VLd. Unequivocal evidence of these neuronal chains await demonstration at the electron microscopic level of synapses between terminals from the associative GPi and retrogradely labelled thalamocortical neurons in the VLd.

The results of the present study provide the first description of the efferent projections of the rostromedial pole of the GPi in primates. The VApC and the VM were found to be the major targets of this part of the GPi. The striatal cells that project to the rostromedial GPi, as mentioned above, receive input from limbic and/or associative cortices. The limbic information from the striatum also reaches the thalamus via a relay in the ventral pallidum or the subcommissural part of the external globus pallidus (GPe; Zahm and Brog, 1992; Haber et al., 1993). In contrast to the rostromedial pole of the GPi, the major thalamic target of the ventral pallidum is the magnocellular region of the mediodorsal nucleus (Zahm and Brog, 1992; Haber et al., 1993), which projects to the anterior orbitofrontal cortex (Goldman-Rakic and Porrino, 1985; Ilinsky et al., 1985; Barbas et al., 1991). On the other hand, the VApC projects to the dorsomedial region of the prefrontal cortex (Kievit and Kuypers, 1977; Goldman-Rakic and Porrino, 1985). Therefore, the limbic information that reaches the ventral striatum may be conveyed to different sectors of the prefrontal cortex, depending on their projection sites in the pallidum (for review, see Joel and Weiner, 1994).

Pallidal inputs to the zona incerta

Injections of BDA into the dorsal one-third (group 3) and the rostromedial pole (group 4) of the GPi led to anterogradely labelled fibers in the dorsal part of the zona incerta. In contrast, this structure remained devoid of anterograde labelling after injections in the sensorimotor territory of the GPi. To our knowledge, the present data provide the first evidence for a direct projection from the GPi to the zona incerta in primates. Although the functional significance of this projection is still speculative, the

fact that it arises mainly from the sector of the GPi that receives inputs from the caudate nucleus (Smith and Parent, 1986), combined with the data demonstrating that the deep and intermediate layers of the superior colliculus are the major targets of γ -aminobutyric acid (GABA)ergic projections from the zona incerta (Araki et al., 1984; Ficalora and Mize, 1989), indicate that the striatopallidum-oculomotor projection may be an additional pathway whereby the basal ganglia control visual saccades in monkeys. In keeping with this, Hikosaka and Wurtz (1983) demonstrated that neurons in the zona incerta, which are spontaneously active, decrease their activity at the beginning of saccades. The relationships between the striatopallidum-oculomotor projections and the striatonigrocollicular projections (Hikosaka and Wurtz, 1983; Hikosaka et al., 1989, 1993; Chevalier and Deniau, 1990) for controlling eye movements remain to be established. Inputs arising from the dorsal and rostromedial parts of the GPi, as was the case at the level of the VA/VL, converged to a common region in the zona incerta.

Pallidal inputs to the CM/PF

One of the major findings of the present study is that the GPi sends a massive projection to the PF in the squirrel monkey. These data extend the previous observations of DeVito and Anderson (1982), who found anterograde labelling in the rostromedial part of the PF after injections of tritiated amino acids in the dorsomedial one-third of the GPi. In contrast, most of the previous studies showed that the GPi efferents were confined to the CM (Nauta and Mehler, 1966; Kuo and Carpenter, 1973; Kim et al., 1976; Parent and DeBellefeuille, 1983; François et al., 1988; Hazrati and Parent, 1991; Page et al., 1993). These findings led to the current view that the CM is the sole intralaminar nucleus that receives inputs from the GPi in primates (Parent, 1990). Our data demonstrate that a projection from the GPi to the PF indeed exists and that this input arises from the associative and limbic territories of the GPi in the squirrel monkey. On the other hand, neurons in the sensorimotor territory of the GPi project exclusively to the CM. These findings are in keeping with observations showing that the PF is the major source of thalamic afferents to the associative and limbic striatal areas, whereas the CM is mainly associated with the sensorimotor part of the striatum in primates (Parent et al., 1983; Smith and Parent, 1986; Sadikot et al., 1989, 1992a,b; François et al., 1991). Therefore, the functional segregation imposed upon the GPi by striatal afferents appears to be maintained at the level of the CM/PF in monkeys.

Another important finding of our study is the existence of a projection from the associative and/or limbic GPi to the so-called PFdl. The labelling in this region was particularly prominent after injections in the dorsal one-third of the GPi. In keeping with these data, DeVito and Anderson (1982) found a band of anterograde labelling in a region that corresponded to that of the PFdl after injections of tritiated amino acids in the dorsomedial part of the GPi in macaques. Because this region was considered to be a part of the CM in previous studies (Parent et al., 1983; Smith and Parent, 1986), the exact region of the striatum that receives input from the PFdl still remains to be established. Future studies combining anterograde labelling from the associative region of the GPi with retrograde labelling from specific functional territories of the striatum

tum, therefore, are essential for a better understanding of the neuronal networks that underlie the integration of the PFdl in the functional organization of the basal ganglia-thalamostriatal circuitry in primates. Preliminary evidence in our laboratory indicates that the PFdl projects preferentially to the precommissural part of the putamen, (Sidibé and Smith, unpublished observation) a region of the striatum that is involved in the preparatory activity related to internal generation of individual behavioral acts (Schultz and Romo, 1992).

Synaptic organization of pallidal inputs to the VA/VL and the CM

The ultrastructure and synaptic organization of GPI terminals in the VLp are in keeping with the findings in cats (Grofova and Rinvik, 1974; Kultas-Ilinsky et al., 1983). The fact that the pallidal boutons form symmetric synapses is consistent with their GABAergic nature (Smith et al., 1987) and the tonic inhibitory effect maintained by the GPI on thalamocortical neurons (for review, see Chevalier and Deniau, 1990). To our knowledge, the only available data relating to the synaptology of GPI terminals in the monkey thalamus were obtained with the anterograde degeneration method (Harding, 1973; Harding and Powell, 1977) and involved large electrolytic lesions of the GPI. These lesions invariably interrupted major descending corticothalamic fibers and led to controversial data regarding the morphology of pallidal terminals. Very few pallidal boutons were found to form synapses with vesicle-filled dendrites in the present study. The presence or absence of synaptic vesicles in dendritic shafts is the criterion for differentiating dendrites of interneurons from those of relay cells in the thalamus (Jones, 1985). On the basis of previous physiological data (Chevalier and Deniau, 1990), as expected, the projection neurons received the bulk of inhibitory inputs from the pallidum (see also Grofova and Rinvik, 1974; Kultas-Ilinsky et al., 1983). In the cat, Kultas-Ilinsky et al. (1983) estimated the proportion of pallidal boutons in contact with vesicle-filled dendrites in the VA/VL at 8%, which is slightly higher than that found in the present study. Species differences between cats and monkeys or differences in the location of the sampling areas may explain this slight discrepancy.

Another output structure of the basal ganglia that projects to the thalamus is the substantia nigra pars reticulata (SNr). Although the afferents from the SNr are largely segregated from those arising from the GPI in the thalamus of primates (for review, see Ilinsky and Kultas-Ilinsky, 1987), the two populations of terminals display common ultrastructural features and follow the same pattern of synaptic innervation in their respective targets (Ilinsky et al., 1982, 1993; Kultas-Ilinsky et al., 1983; Ilinsky, 1990; Kultas-Ilinsky and Ilinsky, 1990). The two output structures of the basal ganglia, therefore, are in positions to control the spread of depolarization from distal dendrites to the somata of thalamocortical cells.

The majority of GPI terminals in the CM were found to display ultrastructural features that resembled those of pallidal boutons in the VLp, except that the pallidal terminals were slightly smaller and less elongated in the CM than in the VLp (see also Grofova and Rinvik, 1974). However, the pattern of distribution of GPI boutons at the level of single neurons was quite similar in both thalamic nuclei. Similarly, the postsynaptic targets contacted by GPI terminals in the CM displayed the ultrastructural

features of projection neurons. The only exception was a rare type of labelled bouton that contained round, synaptic vesicles and formed asymmetric synapses with vesicle-filled dendrites. Although it is unlikely that these boutons arose from the GPI, the fact that very few were encountered indicates that most of the BDA-containing terminals examined in the electron microscope originated from pallidal neurons. In the light of recent findings showing that CM terminals innervate preferentially the striatopallidal cells projecting to the GPI in the squirrel monkey (Sidibé and Smith, 1994; 1996), the results of the present study suggest the existence of a feedback loop between the striato-GPI neurons in the sensorimotor territory of the striatum and the CM-striatal neurons. Anterograde and retrograde tract-tracing experiments at the electron microscopic level are in progress to determine the precise territory of the striatum innervated by the CM, PF, and PFdl neurons contacted by GPI terminals in the squirrel monkey.

CONCLUSIONS

In 1986, Alexander and his colleagues proposed that the information flowing through the basal ganglia-thalamocortical circuitry remains largely segregated in separate channels that include discrete, nonoverlapping parts of the striatum, globus pallidus, thalamus, and cerebral cortex. From the standpoint of information processing, the model proposed by Alexander and colleagues (1986, 1990) suggests that the basal ganglia-thalamocortical circuitry relays unprocessed information around closed and completely isolated loops. In this regard, the authors suggested that structural convergence and functional integration are more likely to occur within than between the separate basal ganglia-thalamocortical circuits (Alexander and Crutcher, 1990). This concept of parallel organization has been challenged by authors who emphasized that the large, disc-like dendritic fields of individual pallidal neurons might receive strong, convergent inputs from different functional regions of the striatum (Percheron and Fillion, 1991). However, because these two seemingly opposing views use different levels of analysis, it is impossible to state on the basis of such data that the information is integrated between, rather than within, circuits. On the other hand, the interaction between different basal ganglia-thalamocortical circuits is essential for producing coherent behavior. Such interactions could take place at different levels, including corticocortical, intrastriatal, and nigrostriatal connections. In a recent review, Joel and Weiner (1994) argued that the basal ganglia-thalamocortical circuits are composed of closed pathways emanating from and terminating in the same cortical region as well as open pathways, which arise from a specific cortical region and terminate in different cortical areas. This model is consistent with the proposal that the organization of the basal ganglia-thalamocortical circuitry is fundamentally interconnected rather than segregated (Joel and Weiner, 1994). For instance, the limbic "split" circuit contains a closed limbic loop that reenters the limbic region of the cerebral cortex and an open limbic pathway that terminates in associative prefrontal regions (Joel and Weiner, 1994). Our findings provide another substrate by which associative and limbic basal ganglia-thalamocortical circuits may interact at the subcortical level. Moreover, the convergence of associative and limbic GPI efferents was not only found at the level of the VA/VL but also occurred in the CM/PF,

the zona incerta, and, as shown in the accompanying paper, in the pedunculo-pontine nucleus (Smith and Shink, 1995; Shink et al., 1997). However, on the basis of our findings, it is impossible to state that single thalamocortical neurons receive inputs from associative and limbic regions of the GPi. Double anterograde labelling studies at the electron microscopic level (Smith and Bolam, 1991, 1992; Smith, 1993) are currently in progress to elucidate this issue.

ACKNOWLEDGMENTS

The authors thank Jean-François Paré and Isabelle Deaudelin for their excellent technical assistance.

Note added to the proof: The ultrastructural features and pattern of synaptic innervation of pallidal terminals in the centromedian nucleus reported in our study are in keeping with recent observations in macaques (Balercia et al. 1996).

LITERATURE CITED

- Alexander, G.E., and M.D. Crutcher (1990) Functional architecture of basal ganglia circuits: Neural substrates of parallel processing. *Trends Neurosci.* *13*:266–271.
- Alexander, G.E., and M.R. DeLong (1985) Microstimulation of the primate neostriatum. II. Somatotopic organization of striatal microexcitable zones and their relation to neuronal response properties. *J. Neurophysiol.* *53*:1417–1430.
- Alexander G.E., M.R. DeLong, and P.L. Strick (1986) Parallel organization of functionally segregated circuits linking basal ganglia and cortex. *Annu. Rev. Neurosci.* *9*:357–381.
- Araki, M., P.L. McGeer, and E.G. McGeer (1984) Presumptive gamma-aminobutyric acid pathways from the midbrain to the superior colliculus studied by a combined horseradish peroxidase- γ -aminobutyric acid transaminase pharmacohistochemical method. *Neuroscience* *13*:433–439.
- Balercia, G., K. Kultas-Ilinsky, M. Bentivoglio, and I.A. Ilinsky (1996) Neuronal and synaptic organization of the centromedian nucleus of the monkey thalamus: a quantitative ultrastructural study, with tract tracing and immunohistochemical observations. *J. Neurocytol.* *25*:267–288.
- Barbas, H., T.H. Haswell Henion, and C.R. Dermon (1991) Diverse thalamic projections to the prefrontal cortex in the rhesus monkey. *J. Comp. Neurol.* *313*:65–94.
- Beckstead, R.M. (1984) The thalamostriatal projection in the cat. *J. Comp. Neurol.* *223*:313–346.
- Brandt, H.M., and A.V. Apkarian (1992) Biotin-dextran: A sensitive anterograde tracer for neuroanatomic studies in rat and monkey. *J. Neurosci. Methods* *45*:35–40.
- Carter, D.A., and H.C. Fibiger (1978) The projections of the entopeduncular nucleus and globus pallidus in rat as demonstrated by autoradiography and horseradish peroxidase histochemistry. *J. Comp. Neurol.* *177*:113–124.
- Chevalier, G., and J.M. Deniau (1990) Disinhibition as a basic process in the expression of striatal functions. *Trends Neurosci.* *13*:277–280.
- Darian-Smith, C., I. Darian-Smith, and S. Cheema (1990) Thalamic projections to sensorimotor cortex in the macaque monkey: Use of multiple retrograde fluorescent tracers. *J. Comp. Neurol.* *299*:17–46.
- DeLong, M.R., and A.P. Georgopoulos (1981) Motor functions of the basal ganglia. In J.M. Brookhart, V.B. Mountcastle, and V.B. Brooks (eds): *Handbook of Physiology, Section 1, The Nervous System, Vol. 2, Motor Control, Part 2*. Bethesda, MD: Am. Physiol. Soc., pp. 1017–1061.
- DeLong, M.R., M.D. Crutcher, and A.P. Georgopoulos (1985) Primate globus pallidus and subthalamic nucleus: Functional organization. *J. Neurophysiol.* *53*:530–543.
- DeVito, J.L., and M.E. Anderson (1982) An autoradiographic study of efferent connections of the globus pallidus in *Macaca mulatta*. *Exp. Brain Res.* *46*:107–117.
- Emmers, R., and K. Akert (1963) *A Stereotaxic Atlas of the Brain of the Squirrel Monkey (*Saimiri sciureus*)*. Madison, WI: University of Wisconsin Press.
- Fénelon, G., C. François, G. Percheron, and J. Yelnik (1990) Topographic distribution of pallidal neurons projecting to the thalamus in macaques. *Brain Res.* *520*:27–35.
- Ficalora, A.S., and R.R. Mize (1989) The neurons of the substantia nigra and zona incerta which project to the cat superior colliculus are GABA immunoreactive: A double-label study using GABA immunocytochemistry and lectin retrograde transport. *Neuroscience* *29*:567–581.
- Flaherty, A.W., and A.M. Graybiel (1991) Corticostriatal transformation in the primate somatosensory system. Projections from physiologically mapped body-part representations. *J. Neurophysiol.* *66*:1249–1263.
- Flaherty, A.W., and A.M. Graybiel (1993) Two input systems for body representations in the primate striatal matrix: Experimental evidence in the squirrel monkey. *J. Neurosci.* *13*:1120–1137.
- François, C., G. Percheron, J. Yelnik, and D. Tandé (1988) A topographic study of the course of nigral axons and of the distribution of pallidal axonal endings in the centre médian-parafascicular complex of macaques. *Brain Res.* *473*:181–186.
- François, C., G. Percheron, A. Parent, A.F. Sadikot, and J. Yelnik (1991) Topography of the projection from the central complex of the thalamus to the sensorimotor striatal territory in monkeys. *J. Comp. Neurol.* *305*:17–34.
- Goldman, P.S., and W.J.H. Nauta (1977) An intricately patterned prefronto-caudate projection in the rhesus monkey. *J. Comp. Neurol.* *171*:369–386.
- Goldman-Rakic, P.S., and L.J. Porrino (1985) The primate mediodorsal nucleus (MD) and its projection to the frontal lobe. *J. Comp. Neurol.* *242*:535–560.
- Gosh, S., C. Brinkman, and R. Porter (1987) A quantitative study of the distribution of neurons projecting to the precentral motor cortex in the monkey (*M. fascicularis*). *J. Comp. Neurol.* *259*:424–444.
- Grofova, I., and E. Rinvik (1974) Cortical and pallidal projections to the nucleus ventralis lateralis thalami. Electron microscopical studies in the cat. *Anat. Embryol.* *146*:113–122.
- Haber, S.N., E. Lynd, C. Klein, and H.J. Groenewegen (1990) Topographic organization of the ventral striatal efferent projections in the rhesus monkey: An anterograde tracing study. *J. Comp. Neurol.* *293*:282–288.
- Haber, S.N., E. Lynd-Balta, and S.J. Mitchell (1993) The organization of the descending ventral pallidal projections in the monkey. *J. Comp. Neurol.* *329*:111–128.
- Haber, S.N., K. Kunishio, M. Mizobuchi, and E. Lynd-Balta (1995) The orbital and medial prefrontal circuit through the primate basal ganglia. *J. Neurosci.* *15*:4851–4867.
- Harding, B.N. (1973) An ultrastructural study of the termination of afferent fibres within the ventrolateral and centre median nuclei of the monkey thalamus. *Brain Res.* *54*:341–346.
- Harding, B.N., and T.P.S. Powell (1977) An electron microscopic study of the centre-median and ventrolateral nuclei of the thalamus in the monkey. *Proc. R. Soc. London* *279*:357–412.
- Harnois, C., and M. Fillion (1982) Pallidofugal projections to thalamus and midbrain: A quantitative antidromic activation study in monkeys and cats. *Exp. Brain Res.* *47*:277–285.
- Hazrati, L.-N., and A. Parent (1991) Contralateral pallidothalamic and pallidotelmental projections in primates: An anterograde and retrograde labeling study. *Brain Res.* *567*:212–223.
- Hikosaka, O., and R.H. Wurtz (1983) Visual and oculomotor functions of monkey substantia nigra pars reticulata. I. Relation of visual and auditory response to saccades. *J. Neurophysiol.* *49*:1230–1253.
- Hikosaka, O., M. Sakamoto, and S. Usui (1989) Functional properties of monkey caudate neurons. I. Activities related to saccadic eye movements. *J. Neurophysiol.* *61*:780–798.
- Hikosaka, O., M. Sakamoto, and N. Miyashita (1993) Effects of caudate nucleus stimulation on substantia nigra cell activity in monkey. *Exp. Brain Res.* *95*:457–472.
- Holsapple, J.W., J.B. Preston, and P.L. Strick (1991) The origin of thalamic inputs to the “hand” representation in the primary motor cortex. *J. Neurosci.* *11*:2644–2654.
- Hoover, J.E., and P.L. Strick (1993) Multiple output channels in the basal ganglia. *Science* *259*:819–821.
- Ilinsky, I.A. (1990) Structural and connective diversity of the primate motor thalamus: Experimental light and electron microscopic studies in the rhesus monkey. *Stereotact. Funct. Neurosurg.* *54*:114–124.
- Ilinsky, I.A., and K. Kultas-Ilinsky (1987) Sagittal cytoarchitectonic maps of the *Macaca mulatta* thalamus with a revised nomenclature of the motor-related nuclei validated by observations on their connectivity. *J. Comp. Neurol.* *262*:331–364.

- Ilinsky, I.A., K. Kultas-Ilinsky, and K.R. Smith (1982) Organization of basal ganglia inputs to the thalamus: A light and electron microscopic study in the cat. *Appl. Neurophysiol.* 45:230–237.
- Ilinsky, I.A., M.L. Jouandet, and P.S. Goldman-Rakic (1985) Organization of the nigrothalamocortical system in the rhesus monkey. *J. Comp. Neurol.* 236:315–330.
- Ilinsky, I.A., W.G. Tourtelotte, and K. Kultas-Ilinsky (1993) Anatomical distinctions between the two basal ganglia afferent territories in the primate motor thalamus. *Stereotact. Funct. Neurosurg.* 60:62–69.
- Inase, M., and J. Tanji (1994) Projections from the globus pallidus to the thalamic areas projecting to the dorsal area 6 of the macaque monkey: A multiple tracing study. *Neurosci. Lett.* 180:135–137.
- Inase, M., and J. Tanji (1995) Thalamic distribution of projection neurons to the primary motor cortex relative to afferent terminal fields from the globus pallidus in the macaque monkey. *J. Comp. Neurol.* 353:415–426.
- Jayaraman (1984) Thalamostriate projections—An overview. In J.S. McKenzie, R.E. Kemm, and L.N. Wilcock (eds): *Basal Ganglia: Structure and Function*. New York: Plenum Press, pp. 69–86.
- Jinnai, K., A. Nambu, I. Tanibuchi, and S.-I. Yoshida (1993) Cerebello- and pallido-thalamic pathways to area 6 and 4 in the monkey. *Stereotact. Funct. Neurosurg.* 60:70–79.
- Joel, D., and I. Weiner (1994) The organization of the basal ganglia-thalamocortical circuits: Open interconnected rather than closed segregated. *Neuroscience* 63:363–379.
- Jones, E.G. (1985) *The Thalamus*. New York: Plenum Press.
- Jürgens, U. (1984) The efferent and afferent connections of the supplementary motor area. *Brain Res.* 300:63–81.
- Kayahara, T., and K. Nakano (1996) Pallido-thalamo-cortical connections: An electron microscopic study in the macaque monkey. *Brain Res.* 706:337–342.
- Kemp, J.M., and T.P.S. Powell (1970) The cortico-striate projection in the monkey. *Brain* 93:525–546.
- Kievit, J., and H.G.J.M. Kuypers (1977) Organization of the thalamocortical connections to the frontal lobe in the rhesus monkey. *Exp. Brain Res.* 29:299–322.
- Kim, R., K. Nakano, A. Jayaraman, and M.B. Carpenter (1976) Projections of the globus pallidus and adjacent structures: An autoradiographic study in the monkey. *J. Comp. Neurol.* 169:263–290.
- Kultas-Ilinsky, K., and I.A. Ilinsky (1990) Fine structure of the magnocellular subdivision of the ventral anterior thalamic nucleus (VAmc) of *Macaca mulatta*: II. Organization of nigrothalamic afferents as revealed with EM autoradiography. *J. Comp. Neurol.* 294:479–489.
- Kultas-Ilinsky, K., I. Ilinsky, S. Warton, and K.R. Smith (1983) Fine structure of nigral and pallidal efferents in the thalamus: An EM autoradiographic study in the cat. *J. Comp. Neurol.* 216:390–405.
- Kunishio, K., and S.N. Haber (1994) Primate cingulo-striatal projection: Limbic striatal vs. sensorimotor striatal input. *J. Comp. Neurol.* 350:337–356.
- Künzle, H. (1975) Bilateral projections from precentral motor cortex to the putamen and other parts of the basal ganglia. An autoradiographic study in *Macaca fascicularis*. *Brain Res.* 88:195–209.
- Künzle, H. (1977) Projections from primary somatosensory cortex to basal ganglia and thalamus in the monkey. *Exp. Brain Res.* 30:481–492.
- Künzle, H., and K. Akert (1977) Efferent connections of cortical area 8 (frontal eye field) in *Macaca fascicularis*. A reinvestigation using the autoradiographic technique. *J. Comp. Neurol.* 173:147–164.
- Kuo, J.-S., and M.B. Carpenter (1973) Organization of pallidothalamic projections in the rhesus monkey. *J. Comp. Neurol.* 151:201–236.
- Larsen, K.D., and J. Sutin (1978) Output organization of the feline entopeduncular and subthalamic nuclei. *Brain Res.* 157:21–31.
- Leichnetz, G.R. (1986) Afferent and efferent connections of the dorsolateral precentral gyrus (area 4, hand/arm region) in the macaque monkey, with comparisons to area 8. *J. Comp. Neurol.* 254:460–492.
- Liles, S.L., and B.V. Updyke (1985) Projections of the digit and wrist area of precentral gyrus to the putamen: Relation between topography and physiological properties of neurons in the putamen. *Brain Res.* 339:245–255.
- Matelli, M., G. Luppino, L. Fofassi, and G. Rizzolatti (1989) Thalamic organization to inferior area 6 and area 4 in the macaque monkey. *J. Comp. Neurol.* 280:468–488.
- Middleton, F.A., and P.L. Strick (1994) Anatomical evidence for cerebellar and basal ganglia involvement in higher cognitive function. *Science* 266:458–461.
- Nakano, K., Y. Hasegawa, T. Kayahara, A. Tokushige, and Y. Kuga (1993) Cortical connections of the motor thalamic nuclei in the Japanese monkey, *Macaca fuscata*. *Stereotact. Funct. Neurosurg.* 60:42–61.
- Nambu, A., S. Yoshida, and K. Jinnai (1988) Projection on the motor cortex of thalamic neurons with pallidal input in the monkey. *Exp. Brain Res.* 71:658–662.
- Nambu, A., S. Yoshida, and K. Jinnai (1991) Movement-related activity of thalamic neurons with input from the globus pallidus and projection to the motor cortex in the monkey. *Exp. Brain Res.* 84:279–284.
- Nauta, H.J.W. (1979) Projections of the pallidal complex: An autoradiographic study in the cat. *Neuroscience* 4:1853–1873.
- Nauta, W.J.H., and W.R. Mehler (1966) Projections of the lentiform nucleus in the monkey. *Brain Res.* 1:3–42.
- Olszewski, J. (1952) *The Thalamus of the Macaca mulatta*. An Atlas for Use With Stereotaxic Instrument. Basel: Karger.
- Page, R.D., M.A. Sambrook, and A.R. Crossman (1993) Thalamotomy for the alleviation of levodopa-induced dyskinesia: Experimental studies in the 1-methyl-4-phenyl-1,2,3,6-tetrahydropyridine-treated Parkinsonian monkey. *Neuroscience* 55:147–165.
- Parent, A. (1990) Extrinsic connections of the basal ganglia. *Trends Neurosci.* 13:254–258.
- Parent, A., and L. DeBellefeuille (1982) Organization of efferent projections from the internal segment of globus pallidus in primate as revealed by fluorescence retrograde labeling method. *Brain Res.* 245:201–213.
- Parent, A., and L. DeBellefeuille (1983) The pallidointralaminar and pallidonigral projections in primate as studied by retrograde double-labeling method. *Brain Res.* 278:11–27.
- Parent, A., A. Mackey, and L. DeBellefeuille (1983) The subcortical afferents to caudate nucleus and putamen in primate: A fluorescence retrograde double labeling study. *Neuroscience* 10:1137–1150.
- Percheron, G., and M. Fillion (1991) Parallel processing in the basal ganglia: Up to a point. *Trends Neurosci.* 14:55–56.
- Reynolds, E.S. (1963) The use of lead citrate at high pH as an electron opaque stain in electron microscopy. *J. Cell. Biol.* 17:208–212.
- Rouiller, E.M., F. Liang, A. Babalian, V. Moret, and M. Wiesendanger (1994) Cerebellothalamic and pallidothalamic projections to the primary and supplementary motor cortical areas: A multiple tracing study in macaque monkeys. *J. Comp. Neurol.* 345:185–213.
- Royce, G.J. (1987) Recent research on the centromedian and the parafascicular nuclei. In M.B. Carpenter and A. Jayaraman (eds): *The Basal Ganglia II: Structure and Function—Current concepts*. New York: Plenum Press, pp. 293–319.
- Royce, G.J., and R.J. Mourey (1985) Efferent connections of the centromedian and parafascicular thalamic nuclei: An autoradiographic investigation in the cat. *J. Comp. Neurol.* 235:277–300.
- Russchen, F.T., I. Bakst, D.G. Amaral, and J.L. Price (1985) The amygdalostriatal projections in the monkey. An anterograde tracing study. *Brain Res.* 329:241–257.
- Sadikot, A.F., C. François, and A. Parent (1989) The centre median and parafascicular thalamic nuclei project respectively to the sensorimotor and associative-limbic striatal territories in the squirrel monkey. *Brain Res.* 510:161–165.
- Sadikot, A.F., A. Parent, and C. François (1992a) Efferent connections of the centromedian and parafascicular thalamic nuclei in the squirrel monkey: A PHA-L study of subcortical projections. *J. Comp. Neurol.* 315:137–159.
- Sadikot, A.F., A. Parent, Y. Smith, and J.P. Bolam (1992b) Efferent connections of the centromedian and parafascicular thalamic nuclei in the squirrel monkey: A light and electron microscopic study of the thalamostriatal projection in relation to striatal heterogeneity. *J. Comp. Neurol.* 320:228–242.
- Sakai, S.T., M. Inase, and J. Tanji (1996) Comparison of cerebellothalamic and pallidothalamic projections in the monkey (*Macaca fuscata*): A double anterograde labeling study. *J. Comp. Neurol.* 368:215–228.
- Schell, G.R., and P.L. Strick (1984) The origin of thalamic inputs to the arcuate premotor and supplementary motor areas. *J. Neurosci.* 4:539–560.
- Schultz, W., and R. Romo (1992) Role of primate basal ganglia and frontal cortex in the internal generation of movements. *Exp. Brain Res.* 91:363–384.
- Selemon, L.D., and P.S. Goldman-Rakic (1985) Longitudinal topography and interdigitation of cortico-striatal projections in the rhesus monkey. *J. Neurosci.* 5:776–794.
- Shindo, K., K. Shima, and J. Tanji (1995) Spatial distribution of thalamic projections to the supplementary motor area and the primary motor

- cortex: A retrograde multiple labeling study in the macaque monkey. *J. Comp. Neurol.* 357:98–116.
- Shink, E., M. Sidibé, and Y. Smith (1997) Efferent connections of the internal globus pallidus in the squirrel monkey: II. Topography and synaptic organization of pallidal efferents to the pedunculopontine nucleus. *J. Comp. Neurol.* 382:348–363.
- Sidibé, M., and Y. Smith (1994) Differential synaptic innervation of striatal neurons projecting to the internal or the external segments of the globus pallidus by thalamic afferents in monkeys. *Soc. Neurosci. Abstr.* 20:783.
- Sidibé, M., and Y. Smith (1996) Differential synaptic innervation of striatofugal neurons projecting to the internal or the external segments of the globus pallidus by thalamic afferents in the squirrel monkey. *J. Comp. Neurol.* 365:445–465.
- Sidibé, M., M.D. Bevan, J.P. Bolam, and Y. Smith (1995) Functional segregation and synaptic organization of the pallidothalamic projection in primates. *Soc. Neurosci. Abstr.* 21:676.
- Smith, Y. (1993) A double anterograde labelling method combining the use of PHA-L and biocytin at electron microscopic level. *Neurosci. Prot.* 93:050-04.
- Smith, Y., and J.P. Bolam (1991) Convergence of synaptic inputs from the striatum and the globus pallidus onto identified nigrocollicular cells in the rat. A double anterograde labeling study. *Neuroscience* 44:45–75.
- Smith, Y., and J.P. Bolam (1992) Combined approaches to experimental neuroanatomy: Combined tracing and immunocytochemical techniques for the study of neuronal microcircuits. In J.P. Bolam (ed): *Experimental Neuroanatomy. A Practical Approach*. Oxford: Oxford University Press, pp. 239–266.
- Smith, Y., and A. Parent (1986) Differential connections of caudate nucleus and putamen in the squirrel monkey (*Saimiri sciureus*). *Neuroscience* 18:347–371.
- Smith, Y., and E. Shink (1995) The pedunculopontine nucleus (PPN): A potential target for the convergence of information arising from different functional territories of the internal pallidum (GPi) in primates. *Soc. Neurosci. Abstr.* 21:677.
- Smith, Y., A. Parent, P. Séguéla, and L. Descarries (1987) Distribution of GABA-immunoreactive neurons in the basal ganglia of the squirrel monkey (*Saimiri sciureus*). *J. Comp. Neurol.* 259:50–65.
- Smith, Y., B.D. Bennett, A. Parent, and A.F. Sadikot (1994) Synaptic relationships between dopaminergic afferents and cortical or thalamic input at the single cell level in the sensorimotor territory of the striatum in monkey. *J. Comp. Neurol.* 344:1–19.
- Stanton, G.B., M.E. Goldberg, and C.J. Bruce (1988) Frontal eye field efferents in the macaque monkey: I. Subcortical pathways and topography of striatal and thalamic terminal fields. *J. Comp. Neurol.* 271:473–492.
- Stepniewska, I., T.M. Preuss, and J.H. Kaas (1994a) Architectonic subdivisions of the motor thalamus of owl monkeys: Nissl, acetylcholinesterase, and cytochrome oxidase patterns. *J. Comp. Neurol.* 349:536–557.
- Stepniewska, I., T.M. Preuss, and J.H. Kaas (1994b) Thalamic connections of the primary motor cortex (M1) of owl monkeys. *J. Comp. Neurol.* 349:558–582.
- Strick, P.L. (1985) How do the basal ganglia and cerebellum gain access to the cortical motor areas? *Behav. Brain Res.* 18:107–123.
- Tokuno, H., and J. Tanji (1993) Input organization of distal and proximal forelimb areas in the monkey primary motor cortex: A retrograde double labeling study. *J. Comp. Neurol.* 333:199–209.
- Tokuno, H., M. Kimura, and J. Tanji (1992) Pallidal inputs to thalamocortical neurons projecting to the supplementary motor area: An anterograde and retrograde double labeling study in the macaque monkey. *Exp. Brain Res.* 90:635–638.
- Van Hoesen, G.W., E.H. Yeterian, and R. Lavizzo-Mourey (1981) Widespread corticostriate projections from temporal cortex of the rhesus monkey. *J. Comp. Neurol.* 199:205–220.
- Veenman, C.L., A. Reiner, and M.G. Honig (1992) Biotinylated dextran amine as an anterograde tracer for single- and double-labeling studies. *J. Neurosci. Methods* 41:239–254.
- Vitek, J.L., J. Ashe, M.R. DeLong, and G.E. Alexander (1994) Physiologic properties and somatotopic organization of the primate motor thalamus. *J. Neurophysiol.* 71:1498–1513.
- Wiesendanger, R., and M. Wiesendanger (1985) The thalamic connections with medial area 6 (supplementary motor cortex) in the monkey (*Macaca fascicularis*). *Exp. Brain Res.* 59:91–104.
- Yeterian, E.H., and D.N. Pandya (1991) Prefrontostriatal connections in relation to cortical architectonic organization in rhesus monkeys. *J. Comp. Neurol.* 312:43–67.
- Yeterian, E.H., and D.N. Pandya (1993) Striatal connections of the parietal association cortices in rhesus monkeys. *J. Comp. Neurol.* 332:175–197.
- Yeterian, E.H., and G.W. Van Hoesen (1978) Cortico-striatal projections in the rhesus monkey: The organization of certain cortico-caudate connections. *Brain Res.* 139:43–63.
- Zahm, D.S., and J.S. Brog (1992) On the significance of subterritories in the "accumbens" part of the rat striatum. *Neuroscience* 50:751–767.
- Zemanick, M.C., P.L. Strick, and R.D. Dix (1991) Direction of transneuronal transport of herpes simplex virus 1 in the primate motor system is strain-dependent. *Proc. Natl. Acad. Sci. USA* 88:8048–8051.